OPTIMAL STATIONKEEP AND ATTITUDE CONTROL OF FLEXIBLE SPACECRAFT

PART I: THEORETICAL DEVELOPMENT

SPAR

SPAR-R.1134 ISSUE A

OPTIMAL STATIONKEEP AND ATTITUDE CONTROL OF FLEXIBLE SPACECRAFT

PART I: THEORETICAL DEVELOPMENT

Prepared for:

DEPARTMENT OF COMMUNICATIONS

Reference:

DSS CONTRACT 15ST.36100-1-0102

OCTOBER, 1982

Spar Aerospace Limited
Remote Manipulator Systems Division
1700 Ormont Drive, Weston, Ontario, Canada M9L 2W7

SPAR Space & Electronics Group

TEL. (416) 745-9680 TELEX 065-27360 SPARORM TOR TWX 610-491-1503 CABLE-SPARORM TOR

Government of Canada / Gouvernement du Canada

Department of Communications

DOC CONTRACTOR REPORT DOC-CR-SP-82-064

DEPARTMENT OF COMMUNICATIONS - OTTAWA - CANADA

SPACE PROGRAM

TITLE: (1) OPTIMAL STATIONKEEP AND ATTITUDE CONTROL OF FLEXIBLE SPACECRAFT --- PART I: THEORETICAL DEVELOPMENT

AUTHOR(S):

J. S-C. Yuan

ISSUED BY CONTRACTOR AS REPORT NO: SPAR-R. 1134

PREPARED BY: Spar Aerospace Ltd.
1700 Ormont Drive,
Weston, Ontario,
Canada M9L 2W7

DEPARTMENT OF SUPPLY AND SERVICES CONTRACT NO: 15ST.36100-1-0102

DOC SCIENTIFIC AUTHORITY: A. H. Reynaud

CLASSIFICATION: Unclassified

DATE: October, 1982

SPAR-R.1134 **ISSUE** A

OPTIMAL STATIONKEEP AND ATTITUDE CONTROL OF FLEXIBLE SPACECRAFT

PART I: THEORETICAL DEVELOPMENT

APPROVALS

R. Ravindran Section Chief, Controls and Analysis
H.F. Barker Manager, Controls and Analysis
S.S. Sachdev Manager, System, Controls and Analysis, Engineering
P.A. McIntyre Director of Engineering

PREPARED BY J. S-C. Yuan, Staff Engineer

REASON FOR RE-ISSUE

DATE October, 1982

AMENDMENTS

NUMBER	REASON FOR AMENDMENT	SIGNATURE	DATE

SPAR FORM 5-22

Spar Aerospace Limited
Remote Manipulator Systems Division
1700 Ormont Drive, Weston, Ontario, Canada M9L 2W7

SPAR Space & Electronics Group

TEL. (416) 745-9680 TELEX 065-27360 SPARORM TOR TWX 610-491-1503 CABLE-SPARORM TOR

PREFACE

This document constitutes the first of two parts of the final report on the work performed by Spar Aerospace Limited under DSS Contract No. 15ST.36100-1-0102, Serial No. OST81-00137.

ABSTRACT

This report describes a method for simultaneously controlling the attitude and orbital position of a flexible spacecraft by means of a combination of thrusters and gimbal actuation. The control algorithm is designed to minimize a quadratic measure of the total control energy and the attitude and position errors.

The dynamical model hierarchy originates from a 73-coordinate model of the spacecraft structural conglomerate. Following model reduction, only 8 rigid modes and 11 elastic modes are retained in the evaluation model; the elastic modes account for up to 99% of the total modal cost. Of the 11 elastic modes, only the four most critical ones, together with the eight rigid modes, are included in the design model.

All the physical coordinates are assumed to be measurable; they comprise the translational and rotational motion of the main bus, the two gimbal angles at the reflector hub, and the relative translation and rotation of the tower tip from the main bus. The thrusters are configured in a way that cross-coupling of control forces and torques is inevitable.

The controller takes the form of linear feedback with constant gains. The gains are calculated off-line from the steady-state solution of a set of Riccati-type equations. The control algorithm sets the gimbal torques and thruster impulses at discrete times.

The variables required for control feedback are obtained via a state estimator. A full-order observer is chosen in lieu of a reduced-order observer in order to minimize the effects of dynamic spillover from the residual modes truncated from the design model. In the case of M-SAT, the 24th-order observer may be decomposed into a 16th-order observer for the rigid modes and a separate 8th-order observer for the elastic modes. The rigid modal observer may be further decoupled into 8 second-order observers, one for each of the rigid modes. Observer complexity is thus greatly reduced.

Finally, the compensator design is modified to accommodate the effects of dynamic spillover from the known residual modes. Control spillover is compensated by appending an additional penalty term to the quadratic performance index. Observation spillover from selected residual modes can be actively suppressed in the elastic modal observer through judicious selection of the observer gains.

The performance of the compensator design will be evaluated via computer simulation in a sequel to this report.

TABLE OF CONTENTS

LIST OF APPENDICES

LIST OF FIGURES

LIST OF TABLES

1.0 INTRODUCTION

Satellites in geosynchronous orbit will gradually drift from a stationary position with respect to an earth-fixed reference frame. Station drift is mainly caused by minor gravitational perturbation of the orbit exerted by the sun and the moon, the oblateness of the earth, and solar radiation pressure acting on large surface areas of the satellite. In spacecraft with momentum storage devices, the use of thrusters for momentum dump could be another cause of station drift. Finally, the actuation of reaction jets during normal mode operations may also induce disturbance acceleration resulting in the spacecraft drifting away from its nominal position.

In conventional satellites, station adjustment - stationkeep - is carried out whenever the drift exceeds a prespecified deadzone defined in terms of latitudinal and longitudinal limits about the nominal position. Typically, thrusters are fired to create linear acceleration in the desired direction to counteract the drift motion. However, due to asymmetric thrusting, plume impingement, and depending on the thruster configuration, thruster actuation is almost always accompanied by torque components which cause rotational motion of the spacecraft. As these thruster-induced disturbance levels are usually very high compared to the environmental disturbances, the attitude control loops must be modified in order to maintain the same pointing accuracy as in the normal mode.

In spacecraft with momentum or reaction wheels, the need to accommodate the stationkeep disturbance torques calls for heavier wheels with the attendant weight penalties. Otherwise, additional thruster actuation may be required in order to maintain the attitude errors within acceptable limits. For the reasons cited earlier, these thruster firings in turn can cause further station drift.

Hence, it can be reasoned that the conventional stationkeep manoeuvre, in which translational motion control is decoupled from attitude control, is probably not the most fuel-efficient approach particularly for spacecraft with a severe thruster asymmetry problem. The primary objective of this study is to investigate a thruster control methodology which simultaneously adjusts the orbital position and controls the attitude of the spacecraft in a fuel-efficient manner.

2.0 SPACECRAFT CONFIGURATION

The spacecraft configuration selected for this study is the Mobile Communications Satellite (M-SAT) shown in Figure 2-1. The main body consists of a bus structure on which is located the bulk of the communications payload as well as various payload support subsystems and a solar array. The boom and tower masts are taken to be Astromasts of appropriate dimensions. The mast hinges at the main body/boom and boom/tower interfaces are assumed to be fixed once the spacecraft is deployed. The possibility of actuating these joint hinges for attitude control will not be considered here.

Antenna orientation can be adjusted with a two degree-of-freedom gimballing mechanism located at the tower/reflector interface. A set of momentum wheels, either skewed or gimballed, serve as actuators during normal mode operations. The antenna gimbal mechanism may be brought in to augment the beam pointing capability, if necessary.

Bipropellant thrusters will be used for momentum dump and stationkeep manoeuvres. An appropriate thruster complement for M-SAT has been selected in Reference 1. Figure 2-2 displays the thruster locations and the directions of thrust acting on the spacecraft, neither of which can be claimed to be optimal in a dynamical sense. Table 2-1 describes the conventional logic for thruster firing during momentum dump and stationkeep manoeuvres. Also displayed in the table are the coupled control torques and translational accelerations generated by the thruster firings. Clearly, from the control dynamical point of view, much of the coupling can be reduced by locating the reflector thrusters at the 'elbow joint' of the boom structure rather than at the hub. However, there are deployment and installation problems attendant with this configuration which are still unresolved at the moment. Hence, we shall adopt the layout in Figure 2-2 as the baseline configuration for our study.

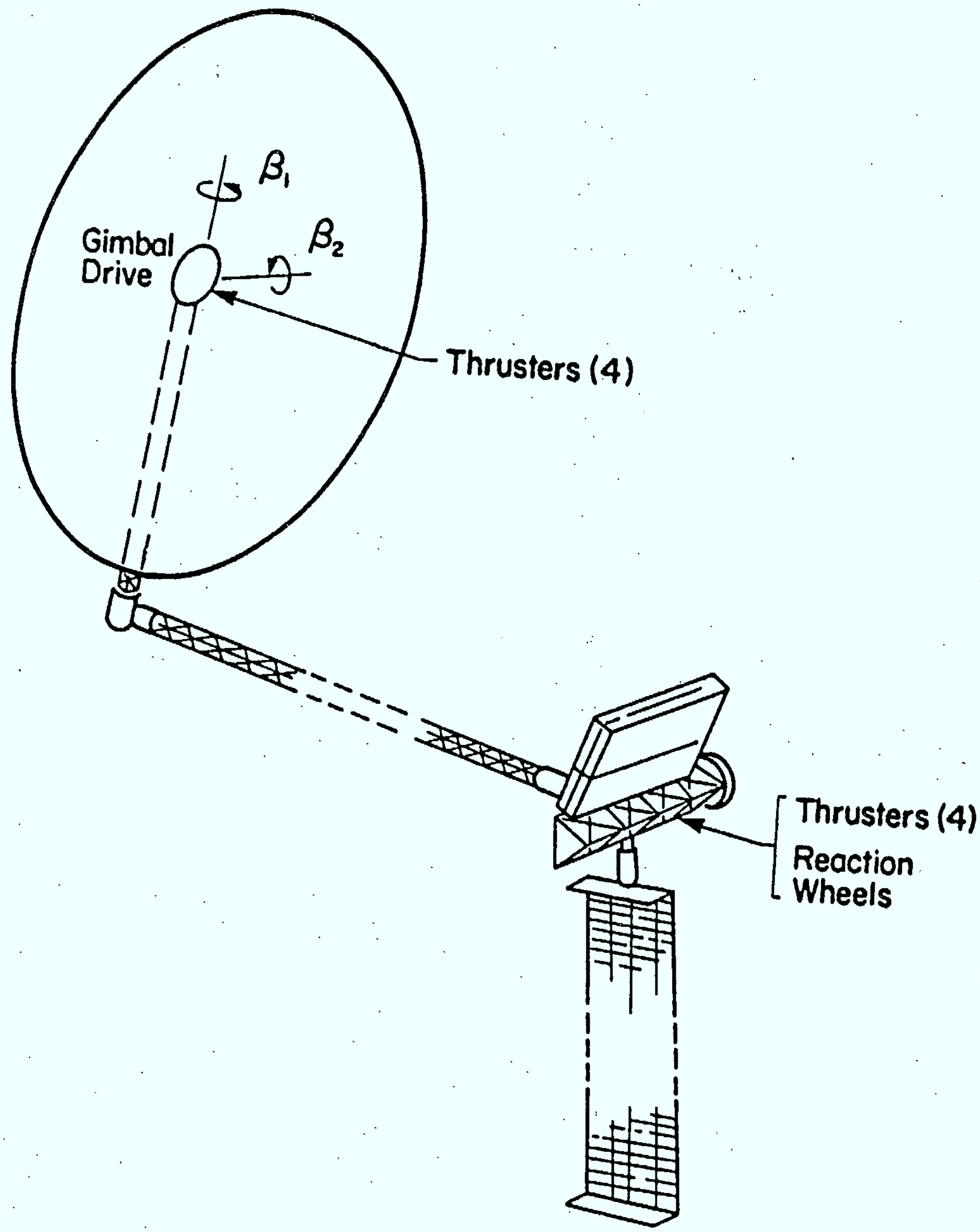

FIGURE 2-1 M-SAT CONFIGURATION LAYOUT

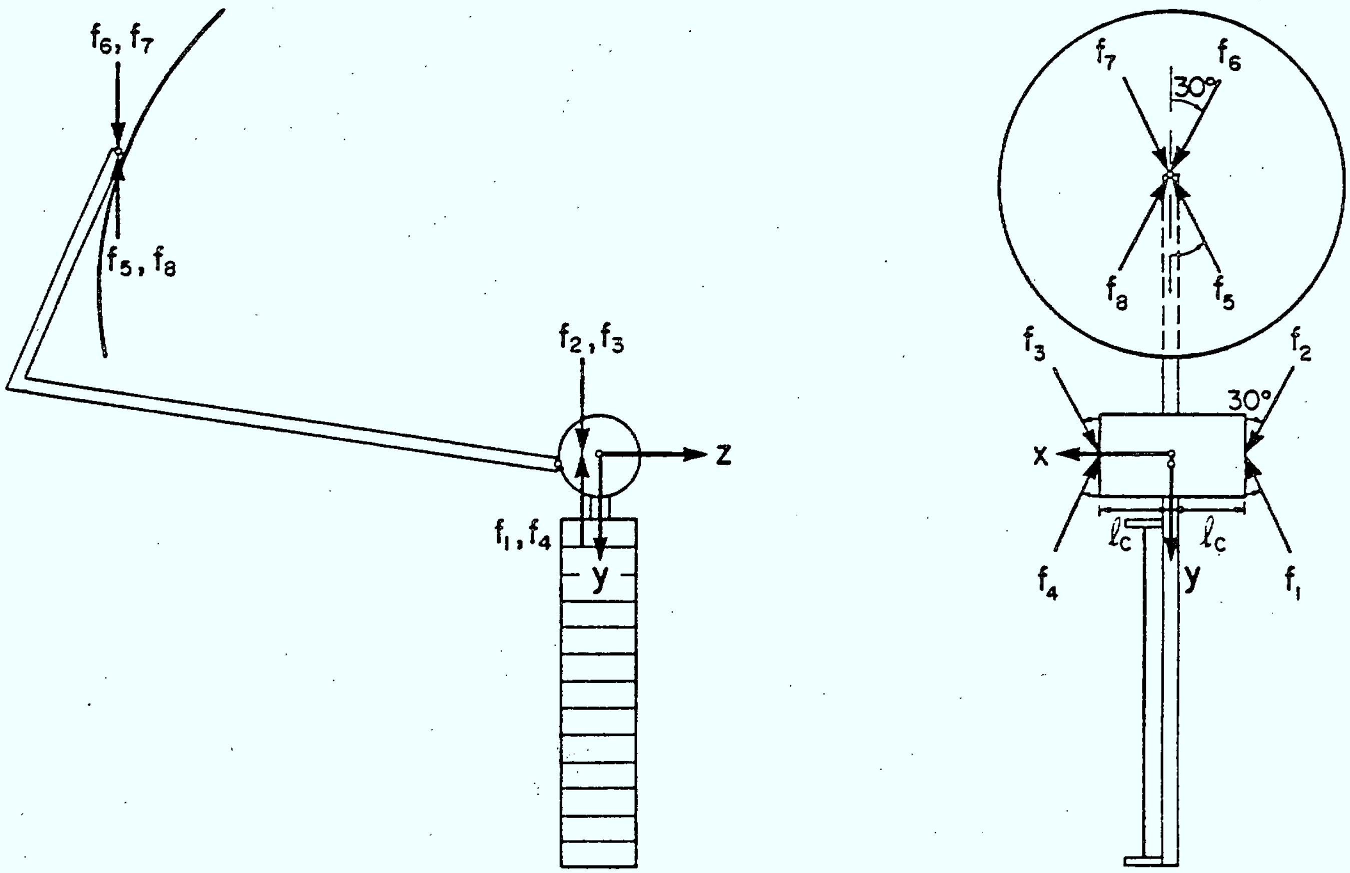

FIGURE 2-2 BASELINE THRUST DIRECTIONS

CONTROL MODE	THRUSTER COMPLEMENT (DUTY CYCLE RATIOS)	AVERAGE TORQUE/D* (N-m)			AV. LIN. ACCELERATION/D (m/s^2)		
		ROLL	PITCH	YAW	N-S	E-W	RADIAL
STATIONKEEP							
North/South	f2,f3,f6,f7 (D/D/0.183D/0.183D)	0.452	0	0	0.0128	0	0
East/West	f1,f2,f5,f6 (D/D/0.183D/0.183D)	0	-0.261	80.32	0	0.00736	0
MOMENTUM DUMP							
+ Roll	f6,f7 (D/D)	1407.98	0	0	0.0108	0	0
- Roll	f5,f8 (D/D)	-1407.98	0	0	-0.0108	0	0
+ Pitch	f1,f8 (D/0.183D)	-0.226	148.63	61.4	-0.00638	0	0
- Pitch	f4,f5 (D/0.183D)	-0.226	-148.63	-61.4	-0.00638	0	0
+ Yaw	f1,f5 (D/0.183D)	-0.226	-0.13	154.5	-0.00638	0.00368	0
- Yaw	f4,f8 (D/0.183D)	-0.226	0.13	-154.48	-0.00638	-0.00368	0

* D: Nominal duty cycle

ASSUMPTIONS:- 22-N thrusters
- Spacecraft mass 3535 Kg
- All dimensions based on SPAR-R.1113
- Perfect thruster alignment & synchronized firing
- All torques referred to nominal centre-of-mass of spacecraft

TABLE 2-1 AVERAGE TORQUES AND LINEAR ACCELERATIONS GENERATED BY THRUSTERS DURING CONVENTIONAL STATIONKEEP AND MOMENTUM DUMP MANOEUVRES

As an illustration, let us consider north-south stationkeep. The thrust impulse required to bring about a change of $\delta\theta$ deg in the orbit inclination is given approximately by

$$F \delta t = m R \omega_0 \left(\frac{\pi}{180}\right) \delta\theta \qquad (2\text{-}1)$$

where m is the mass of the spacecraft, R is the orbit radius and ω_0 is the orbital rate. In the case of M-SAT, m = 3535 Kg and we have

$$F \delta t = 189511.66 \ \delta\theta \quad \text{N-s}$$

From the data in Table 2-1, the perturbation in angular momentum about the roll axis is given by

$$\left|\Delta h_{roll}\right| = \frac{(0.452)(189511.66)}{(0.0128)(3535)} \delta\theta \quad \text{N-m-s}$$

$$= 1893.11 \ \delta\theta \quad \text{N-m-s} \qquad (2\text{-}2)$$

Typically, $\delta\theta$ is 0.1 deg so that the momentum perturbation is about 189 N-m-s, which exceeds the total angular momentum capacity (150 N-m-s) sized for normal mode operations (cf. Reference 2).

The situation during east-west stationkeep is considerably more drastic. Suppose due to the earth oblateness, there is a constant transverse acceleration of $\ddot{\alpha}_0$ deg/s^2 acting to drive the spacecraft in the westward direction. Let the longitudinal deadband be defined as $\pm \alpha_0$ deg about the nominal longitude. When the spacecraft reaches the western edge of the deadband, the conventional stationkeep strategy is to introduce an initial drift rate (say, $\dot{\alpha}_0$ deg/s) in the easterly direction whose magnitude is just large enough to cause the spacecraft to drift to a halt at the eastern edge of the deadband. During the remaining half of the stationkeep cycle, the environmental acceleration is left to drive the spacecraft back to the western edge at which point the next stationkeep manoeuvre is initiated.

The position of the spacecraft, as measured from the nominal longitude, at any time after its departure from the western edge of the deadband is given by

$$\alpha(t) = -\alpha_0 + \dot{\alpha}_0 t - \ddot{\alpha}_0 t^2/2 \quad \text{deg} \qquad (2\text{-}3)$$

It is easily shown that in order for the spacecraft to drift to a halt after T seconds, the initial drift rate must be

$$\dot{\alpha}_0 = \ddot{\alpha}_0 T \quad \text{deg/s}$$

Furthermore, T is given by

$$T = 2\sqrt{\alpha_0/\ddot{\alpha}_0} \quad \text{s} \qquad (2\text{-}4)$$

so that,

$$\dot{\alpha}_0 = 2\sqrt{\alpha_0 \ddot{\alpha}_0} \quad \text{deg/s} \qquad (2\text{-}5)$$

The spacecraft will thus be drifting at a rate of $\dot{\alpha}_0$ in the westward direction when it returns to the western edge of the deadband after 2T seconds. In order to cause a net drift rate of $\dot{\alpha}_0$ in the easterly direction, the thruster firings must be timed to cause a net change in the drift rate of magnitude

$$\Delta\dot{\alpha} = 2\dot{\alpha}_0 = 4\sqrt{\alpha_0 \ddot{\alpha}_0} \quad \text{deg/s} \qquad (2\text{-}6)$$

Some typical values for α_0 and $\ddot{\alpha}_0$ are

$$\alpha_0 = 0.05 \text{ deg}$$

$$\ddot{\alpha}_0 = 5 \times 10^{-4} \text{ deg/day}^2$$

Thus, the east-west stationkeep cycle time is given by (2-4) as

$$2T = 40 \text{ days}$$

From (2-6), the required change in drift rate is

$$\Delta\dot{\alpha} = 0.02 \text{ deg/day}$$

Based on the information in Table 2-1, this corresponds to momentum perturbations about the pitch and yaw axes of the following magnitudes:

$$\begin{aligned} |\Delta h_{pitch}| &= (0.261)\left[\frac{(0.02)(42238)(10^3)}{(24)(3600)(0.00736)}\right]\frac{\pi}{180} \quad \text{N-m-s} \\ &= (0.261)\ (23.19) \ \text{N-m-s} \\ &= 6.052 \ \text{N-m-s} \\ |\Delta h_{yaw}| &= (80.32)\ (23.19)\ \text{N-m-s} \\ &= 1862.6 \ \text{N-m-s} \end{aligned}$$

The momentum perturbation about the yaw axis is clearly unacceptable.

It is now obvious that the conventional stationkeep strategy will not be feasible for a spacecraft with the configuration of M-SAT. In the remainder of this report we shall develop a control strategy which automatically selects the optimal thruster combination and duty cycles to achieve simultaneous stationkeep and attitude control. Optimality here is defined in terms of fuel consumption (i.e., total thrust impulse) as well as attitude and position errors. Momentum dump could be treated in a similar fashion but will not be addressed in this study.

3.0 DYNAMIC MODEL

3.1 Model Description

The dynamical model of the spacecraft based on which the control system will be designed originated from the 'pre-design' model discussed in Reference 3. The preliminary model carried the following assumptions:

(a) The spacecraft is composed of three flexible structures: a reflector, a solar array and a boom/tower structure, configured with respect to an earth-fixed reference frame as in Figure 3-1.

(b) The reflector is modelled by one (first torsional) mode.

(c) The solar array is modelled by three structural modes: first in-plane, out-of-plane and torsional.

(d) The boom/tower structure is modelled only by its stiffness, although the mass is included in the overall mass matrix of the spacecraft. The structural deformation is characterized by the relative displacement and orientation of the tower tip from the main bus.

Since the appearance of Reference 3, major revisions to the pre-design model have occurred, culminating in the model described in Reference 4 which greatly exceeds the pre-design model in both complexity and fidelity. Among the improvements to the early model are the following:

(a) The tower supporting the reflector is no longer required to be perpendicular to the boom attachment on the main bus (cf. Figure 3-2). In fact, the latter can now lie at an arbitrary angle to the orbital plane.

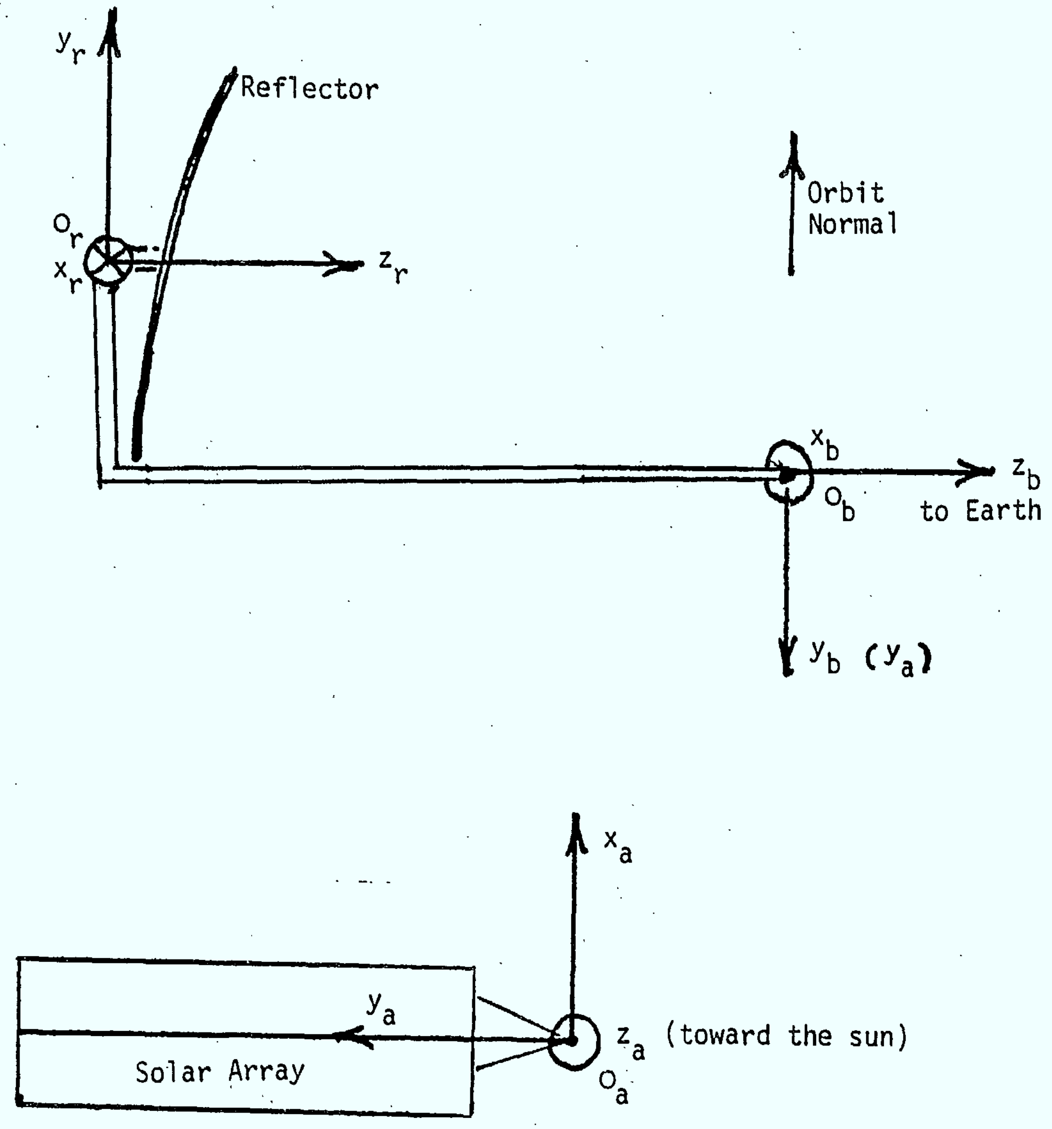

FIGURE 3-1

SPACECRAFT CONFIGURATION FOR PRE-DESIGN MODEL
(TAKEN FROM DYNACON REPORT MSAT-1)

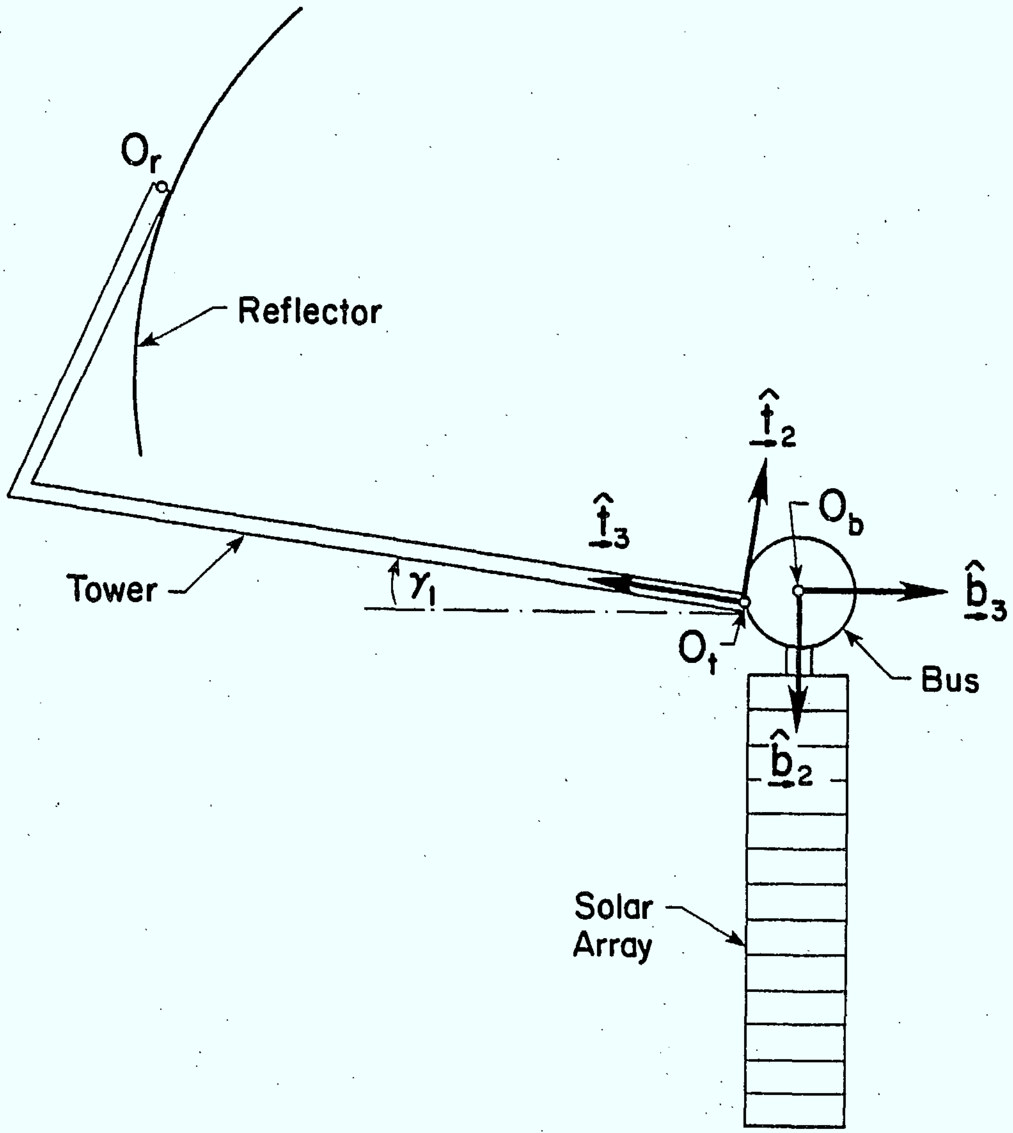

FIGURE 3-2 SPACECRAFT CONFIGURATION FOR DESIGN AND EVALUATION MODELS (TAKEN FROM DYNACON REPORT MSAT-4)

(b) The reflector model is taken from the Jet Propulsion Laboratory's version of a Lockheed wrap-rib reflector which contains data for the first 42 modes of a model with 26,000 degrees of freedom.

(c) The solar array model is essentially Spar's L-SAT array model with 38 modes.

(d) Two models for the boom/tower structure are now available depending on whether one or two elements are used to model each of the tower and boom segments. The more elaborate two-element (four elements for the boom/tower combination) model contains 14 internal elastic coordinates.

Thus, the complete dynamical model for the spacecraft consists of 14 physical coordinates and 94 modal coordinates for a total of 108 degrees of freedom. These coordinates are distributed as follows:

(a) Physical coordinates

$q_1\ q_2\ q_3$ / $q_4\ q_5\ q_6$ — absolute — translation / rotation — of main bus

$q_7\ q_8$ — gimbal angles at the reflector hub

$q_9\ q_{10}\ q_{11}$ / $q_{12}\ q_{13}\ q_{14}$ — relative — translation / rotation — of tower tip from main bus

These are known as physical coordinates because they represent variables which are, in principle, physically measurable. Only q_1 — q_8 represent the rigid body coordinates of the spacecraft.

(b) Modal coordinates

q_a : A 38-dimensional vector containing the elastic coordinates of the solar array

q_i : A 14-dimensional vector containing the elastic coordination of the boom/tower structure

q_r : A 42-dimensional vector containing the elastic coordinates of the reflector

These represent the internal elastic coordinates of the spacecraft.

3.2 Model Truncation

The dynamical equations for the spacecraft can be written in the familiar form

$$M\ddot{q} + C\dot{q} + Kq = Bu \qquad (3\text{-}1)$$

where M is the mass matrix, C is the damping matrix, K is the stiffness matrix and B is the input distribution matrix. Any gyroscopic damping terms may be appended into the C matrix if necessary, but will be ignored in this study.

The coordinates are represented in the vector q as follows:

$$q^T = (q_1 \; \cdots \; q_{14} \;\; q_a^T \;\; q_i^T \;\; q_r^T) \qquad (3\text{-}2)$$

The control input vector u contains the two gimbal torques as well as the eight force terms from the thrusters.

For the purpose of control design and evaluation, a model with such a high degree of fidelity is not warranted. In practice, a majority of the modes will lie beyond the bandwidths of the sensors, the actuators and the compensators, and are therefore 'invisible' as far as the control system is concerned. The dynamical model should then be truncated to retain only the 'important' modes; these could be selected, for instance, on the basis of their contributions to a predefined measurement index. One such idea, the modal penalty index, was used in Reference 3 as a criterion for modal truncation.

As outlined in Reference 5, the model was reduced in two stages. From modal momentum and frequency considerations, the number of the elastic coordinates in the reflector and the array were first reduced from 42 and 38 to 18 and 27, respectively. The model now has a total of 73 coordinates.

Next the q-coordinates are transformed into spacecraft modal (η) coordinates via the transformation

$$q = E\eta \tag{3-3}$$

where the matrix E satisfies the relationships

$$E^T M E = I \quad ; \quad E^T K E = \Omega^2 \tag{3-4}$$

Here I denotes the identity matrix, and Ω^2 is a diagonal matrix whose diagonal elements (except the first eight zeros) are the squares of the natural modal frequencies. Equation (3-1) is now transformed into

$$\ddot{\eta} + \hat{C}\dot{\eta} + \Omega^2\eta = \hat{B}u \tag{3-5}$$

in which the coordinates can be partitioned as

$$\eta^T = (\eta_r^T \ \eta_e^T) \tag{3-6}$$

The vector η_r contains the eight rigid body modes of the spacecraft, while η_e is a 65-vector of the elastic modes. The new damping and input matrices have been transformed as follows

$$\hat{C} = E^T C E \quad ; \quad \hat{B} = E^T B \tag{3-7}$$

where $\hat{C}$ now has the form

$$\hat{C} = \begin{bmatrix} 0 & 0 \\ 0 & \hat{C}_e \end{bmatrix} \tag{3-8}$$

Finally, with the aid of modal cost analysis, the 65 modes in η_e were further reduced to include only the 11 modes with the highest modal costs (cf. Reference 5). Together with the eight rigid body modes, these elastic modes form a 19-mode model which will be used for control evaluation in this study. For control design, only the four modes with the highest modal costs in η_e will be retained. Thus, the design model is now left with a total of 12 modes. Figure 3-3 contains a summary of the truncation process just described.

The numerical values for the matrices E, $\hat{B}$, $\hat{C}$ and Ω^2 for the 'Operational' M-SAT (cf. Reference 1) are listed in Table 3-1.

3.3 Design and Evaluation Models

The equations for the control design and evaluation models will now be stated explicitly. We begin with the evaluation model where, as in (3-6), the modal coordinates are partitioned as

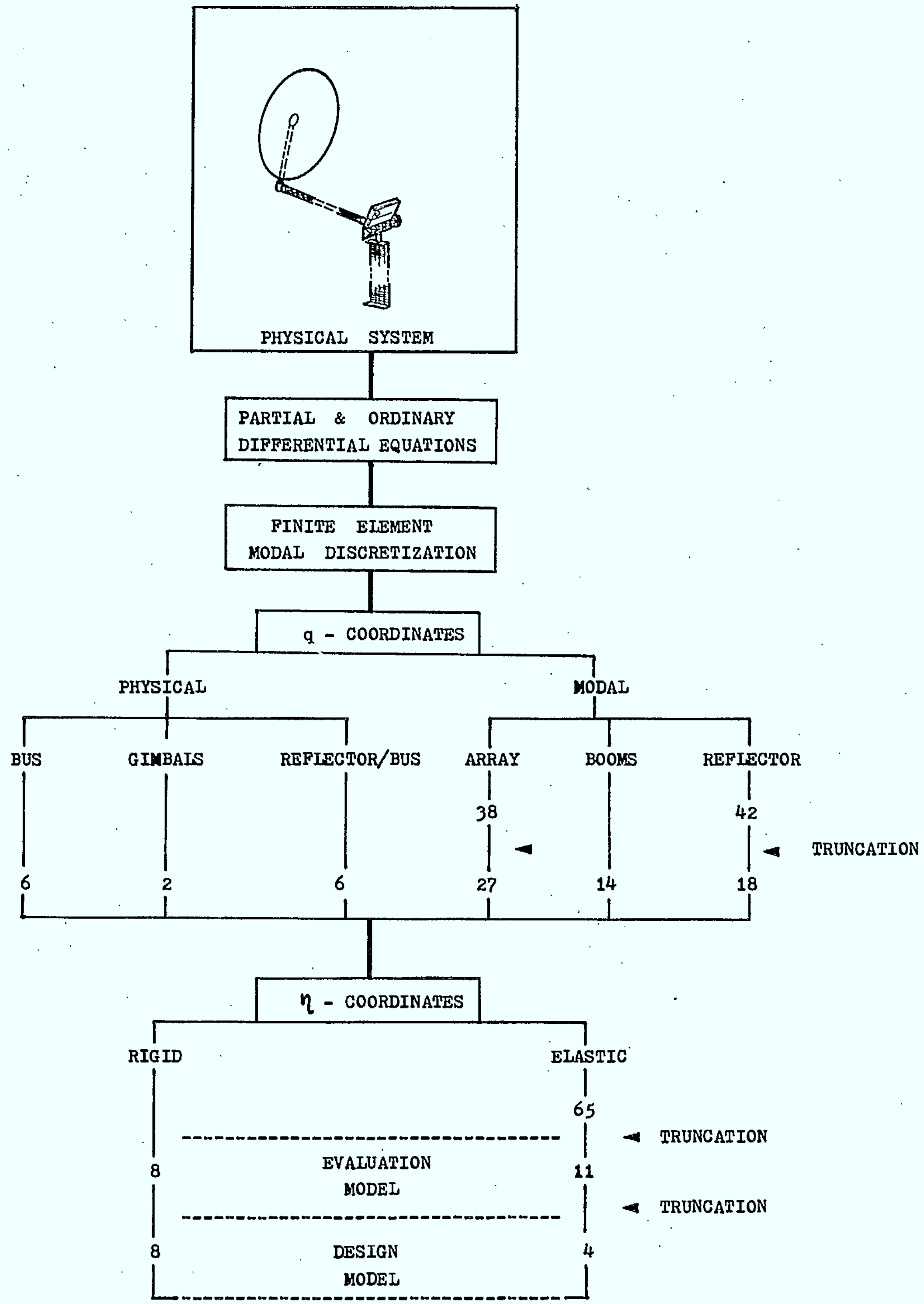

FIGURE 3-3 MODEL HIERARCHY

a) Diagonal Elements of Ω

*** RETAINED FREQUENCIES ***

SELECTED MODES	FREQUENCY (RAD/SEC)	FREQUENCY (HZ)
1	0.0000000000000000D-01	0.0000000000000000D-01
2	0.0000000000000000D-01	0.0000000000000000D-01
3	0.0000000000000000D-01	0.0000000000000000D-01
4	0.0000000000000000D-01	0.0000000000000000D-01
5	0.0000000000000000D-01	0.0000000000000000D-01
6	0.0000000000000000D-01	0.0000000000000000D-01
7	0.0000000000000000D-01	0.0000000000000000D-01
8	0.0000000000000000D-01	0.0000000000000000D-01
9	1.2434952868889490D-01	1.9790842161985070D-02
$\boxed{10}$	1.5117997270041770D-01	2.4061039951769270D-02
11	2.3952489001995300D-01	3.8121570240218110D-02
12	5.5629553169353050D-01	8.8537183688959500D-02
$\boxed{13}$	6.9020123559092970D-01	1.0984893837243020D-01
14	7.7963639163821000D-01	1.2408298554354990D-01
$\boxed{15}$	1.5532815257821910D 00	2.4721243284155700D-01
$\boxed{16}$	3.1368829630482690D 00	4.9925042946988320D-01
$\boxed{17}$	3.9572089569016590D 00	6.2980936633842200D-01
$\boxed{18}$	9.9489251639172970D 00	1.5834206182887820D 00
$\boxed{19}$	1.4008315775600510D 01	2.2294927000789990D 00

$\square$ MODES TRUNCATED FROM DESIGN MODEL

b) Elastic Component of Damping Matrix $\hat{C}$

$$\hat{C} = \begin{bmatrix} 0 & 0 \\ 0 & \hat{C}_e \end{bmatrix}$$

*** RETAINED MODAL DAMPING MATRIX ***

ROW \ COL	1	$\boxed{2}$	3	4	$\boxed{5}$	6
1	1.846D-03	-5.509D-06	2.519D-06	-1.700D-03	1.237D-03	3.255D-03
$\boxed{2}$	-5.509D-06	1.706D-03	3.644D-04	2.246D-05	-1.446D-05	-2.771D-05
3	2.519D-06	3.644D-04	3.409D-03	-6.900D-06	5.243D-06	1.146D-05
4	-1.700D-03	2.246D-05	-6.900D-06	1.711D-02	-6.647D-03	-4.585D-03
$\boxed{5}$	1.237D-03	-1.446D-05	5.243D-06	-6.647D-03	1.109D-02	5.880D-03
6	3.255D-03	-2.771D-05	1.146D-05	-4.585D-03	5.880D-03	4.215D-02
$\boxed{7}$	4.718D-05	-3.210D-03	-8.921D-03	-2.764D-05	7.188D-05	6.426D-04
$\boxed{8}$	1.500D-03	-1.495D-05	7.907D-08	-1.707D-03	2.124D-03	1.163D-02
$\boxed{9}$	1.057D-05	2.151D-03	6.351D-03	-2.617D-05	2.508D-05	7.470D-05
$\boxed{10}$	-1.173D-03	1.330D-05	-7.460D-06	4.837D-03	-2.683D-04	2.760D-02
$\boxed{11}$	-2.607D-03	2.564D-05	-3.086D-05	8.077D-03	-1.308D-03	3.694D-02

ROW \ COL	$\boxed{7}$	$\boxed{8}$	$\boxed{9}$	$\boxed{10}$	$\boxed{11}$
1	4.718D-05	1.500D-03	1.057D-05	-1.173D-03	-2.607D-03
$\boxed{2}$	-3.210D-03	-1.495D-05	2.151D-03	1.330D-05	2.564D-05
3	-8.921D-03	7.907D-08	6.351D-03	-7.460D-06	-3.086D-05
4	-2.764D-05	-1.707D-03	-2.617D-05	4.837D-03	8.077D-03
$\boxed{5}$	7.188D-05	2.124D-03	2.508D-05	-2.683D-04	-1.308D-03
6	6.426D-04	1.163D-02	7.470D-05	2.760D-02	3.694D-02
$\boxed{7}$	1.501D-01	3.174D-04	-8.721D-02	5.814D-04	6.131D-04
$\boxed{8}$	3.174D-04	5.610D-02	-2.360D-05	-1.229D-01	-1.896D-01
$\boxed{9}$	-8.721D-02	-2.360D-05	1.056D-01	6.325D-05	-1.322D-04
$\boxed{10}$	5.814D-04	-1.229D-01	6.325D-05	1.055D 00	1.446D 00
$\boxed{11}$	6.131D-04	-1.896D-01	-1.322D-04	1.446D 00	2.342D 00

$\square$ MODES TRUNCATED FROM DESIGN MODEL

TABLE 3-1

EVALUATION MODEL PARAMETERS FOR OPERATIONAL M-SAT (TAKEN FROM REF. 5)

c) Control Distribution Matrix $\hat{B}$

$$\hat{B} = \begin{bmatrix} \hat{B}_g & \hat{B}_t \end{bmatrix}$$

*** RETAINED MODAL CONTROL DISTRIBUTION MATRIX ***

Gimbal torque input matrix:

$\hat{B}_g$

ROW \ COL		
1	0.000D-01	0.000D-01
2	0.000D-01	0.000D-01
3	0.000D-01	0.000D-01
4	0.000D-01	0.000D-01
5	0.000D-01	0.000D-01
6	0.000D-01	0.000D-01
7	6.944D-03	0.000D-01
8	6.791D-08	6.921D-03
9	-5.553D-04	-2.199D-06
$\boxed{10}$	5.403D-06	-6.851D-04
11	-1.500D-06	-2.577D-03
12	8.518D-04	1.731D-06
$\boxed{13}$	1.688D-05	-8.184D-07
14	4.838D-03	-2.422D-06
$\boxed{15}$	8.906D-05	-2.665D-03
$\boxed{16}$	-1.641D-02	-3.707D-06
$\boxed{17}$	9.890D-06	-5.304D-03
$\boxed{18}$	1.197D-01	-9.102D-07
$\boxed{19}$	1.803D-01	2.451D-04

Thruster force input matrices:

$\hat{B}_t$ - thrusters on bus

ROW \ COL				
1	8.410D-03	8.410D-03	-8.410D-03	-8.410D-03
2	-1.457D-02	1.457D-02	1.457D-02	-1.457D-02
3	0.000D-01	0.000D-01	0.000D-01	0.000D-01
4	5.729D-03	-5.729D-03	-5.729D-03	5.729D-03
5	3.806D-03	3.811D-03	-3.806D-03	-3.811D-03
6	1.022D-02	-7.078D-03	7.133D-03	-1.027D-02
7	1.289D-03	4.539D-05	-4.112D-05	-1.293D-03
8	-8.075D-04	8.081D-04	8.094D-04	-8.100D-04
9	6.530D-03	-3.478D-03	3.488D-03	-6.539D-03
$\boxed{10}$	1.044D-03	-1.055D-03	-1.175D-03	1.186D-03
11	-3.368D-03	3.370D-03	3.419D-03	-3.421D-03
12	-2.485D-02	2.639D-02	-2.653D-02	2.499D-02
$\boxed{13}$	1.358D-02	-1.328D-02	1.336D-02	-1.365D-02
14	-6.475D-04	-3.014D-03	3.025D-03	6.358D-04
$\boxed{15}$	4.183D-03	-4.251D-03	-4.594D-03	4.662D-03
$\boxed{16}$	-1.505D-03	9.903D-04	-1.007D-03	1.521D-03
$\boxed{17}$	-1.833D-03	1.826D-03	2.062D-03	-2.055D-03
$\boxed{18}$	-5.342D-04	6.243D-04	-6.283D-04	5.383D-04
$\boxed{19}$	3.438D-04	-3.829D-04	4.334D-04	-3.943D-04

$\hat{B}_t$ - thrusters at hub

ROW \ COL				
1	8.410D-03	8.410D-03	-8.410D-03	-8.410D-03
2	-1.457D-02	1.457D-02	1.457D-02	-1.457D-02
3	0.000D-01	0.000D-01	0.000D-01	0.000D-01
4	-2.869D-02	2.869D-02	2.869D-02	-2.869D-02
5	-1.906D-02	-1.908D-02	1.906D-02	1.908D-02
6	9.299D-03	9.284D-03	-9.299D-03	-9.284D-03
7	-2.675D-04	-2.702D-04	2.675D-04	2.702D-04
8	9.735D-04	-9.725D-04	-9.735D-04	9.725D-04
9	-4.826D-02	-4.783D-02	4.826D-02	4.783D-02
$\boxed{10}$	-5.105D-02	5.178D-02	5.105D-02	-5.178D-02
11	-1.087D-01	1.085D-01	1.087D-01	-1.085D-01
12	5.095D-02	5.079D-02	-5.095D-02	-5.079D-02
$\boxed{13}$	-4.925D-02	-4.909D-02	4.925D-02	4.909D-02
14	-2.418D-01	-2.413D-01	2.418D-01	2.413D-01
$\boxed{15}$	2.639D-01	-2.724D-01	-2.639D-01	2.724D-01
$\boxed{16}$	3.403D-01	3.403D-01	-3.403D-01	-3.403D-01
$\boxed{17}$	-4.154D-01	4.144D-01	4.154D-01	-4.144D-01
$\boxed{18}$	-2.861D 00	-2.862D 00	2.861D 00	2.862D 00
$\boxed{19}$	-4.259D 00	-4.278D 00	4.259D 00	4.278D 00

$\boxed{}$ MODES TRUNCATED FROM DESIGN MODEL

TABLE 3-1 --CONTINUED

d) First 14 Rows of Coordinate Transformation Matrix E

*** RETAINED EIGENVECTORS ***

ROW \ COL	1	2	3	4	5	6
1	1.682D-02	0.000D-01	0.000D-01	0.000D-01	7.617D-03	3.139D-03
2	0.000D-01	1.682D-02	0.000D-01	-6.615D-03	2.807D-06	3.172D-05
3	0.000D-01	0.000D-01	1.682D-02	9.961D-04	-1.348D-05	-1.016D-05
4	0.000D-01	0.000D-01	0.000D-01	9.094D-04	-3.859D-07	-9.257D-07
5	0.000D-01	0.000D-01	0.000D-01	0.000D-01	1.047D-03	7.331D-04
6	0.000D-01	0.000D-01	0.000D-01	0.000D-01	0.000D-01	2.003D-03
7	0.000D-01	0.000D-01	0.000D-01	0.000D-01	0.000D-01	0.000D-01
8	0.000D-01	0.000D-01	0.000D-01	0.000D-01	0.000D-01	0.000D-01
9	0.000D-01	0.000D-01	0.000D-01	0.000D-01	0.000D-01	0.000D-01
10	0.000D-01	0.000D-01	0.000D-01	0.000D-01	0.000D-01	0.000D-01
11	0.000D-01	0.000D-01	0.000D-01	0.000D-01	0.000D-01	0.000D-01
12	0.000D-01	0.000D-01	0.000D-01	0.000D-01	0.000D-01	0.000D-01
13	0.000D-01	0.000D-01	0.000D-01	0.000D-01	0.000D-01	0.000D-01
14	0.000D-01	0.000D-01	0.000D-01	0.000D-01	0.000D-01	0.000D-01

ROW \ COL	7	8	9	$\boxed{10}$	11	12
1	1.334D-03	5.777D-07	3.051D-03	-1.135D-05	1.986D-06	1.541D-03
2	2.464D-06	9.338D-04	5.393D-06	-1.287D-03	3.920D-03	-8.289D-05
3	-1.609D-06	-2.016D-04	3.738D-05	5.527D-03	4.209D-03	-5.252D-06
4	-9.174D-08	-4.708D-05	-8.282D-07	-3.625D-04	-9.888D-04	8.859D-07
5	1.210D-04	1.119D-07	-5.856D-04	3.905D-06	2.133D-07	-3.964D-04
6	1.441D-04	2.213D-07	1.157D-03	-1.515D-05	5.812D-06	-5.932D-03
7	6.944D-03	6.791D-08	-5.553D-04	5.403D-06	-1.500D-06	8.518D-01
8	0.000D-01	6.921D-03	-2.199D-06	-6.851D-04	-2.577D-03	1.731D-06
9	0.000D-01	0.000D-01	-7.672D-02	6.574D-04	-1.386D-04	1.218D-01
10	0.000D-01	0.000D-01	-1.057D-04	-2.616D-02	-2.193D-02	-5.374D-05
11	0.000D-01	0.000D-01	9.647D-05	2.728D-02	7.066D-02	-4.218D-05
12	0.000D-01	0.000D-01	4.200D-06	1.211D-03	3.425D-03	-2.497D-06
13	0.000D-01	0.000D-01	5.736D-05	-2.287D-06	1.776D-06	-1.050D-03
14	0.000D-01	0.000D-01	3.335D-03	-3.071D-05	8.002D-06	-6.323D-03

ROW \ COL	$\boxed{13}$	14	$\boxed{15}$	$\boxed{16}$	$\boxed{17}$	$\boxed{18}$
1	2.933D-04	-3.661D-03	-6.865D-05	-5.147D-04	-7.681D-06	9.009D-05
2	4.152D-05	6.760D-06	-5.107D-03	-9.540D-06	2.245D-03	-2.352D-06
3	1.037D-05	6.496D-05	-6.523D-04	7.605D-06	5.077D-04	1.096D-06
4	-1.407D-06	-4.329D-06	9.650D-03	3.582D-06	-6.085D-03	1.817D-06
5	-3.743D-04	-5.918D-03	-1.270D-04	-2.459D-03	2.712D-06	-5.308D-04
6	3.110D-03	2.746D-04	-4.746D-05	-2.900D-04	2.644D-05	-1.342D-04
7	1.688D-05	4.838D-03	8.906D-05	-1.641D-02	9.890D-06	1.197D-01
8	-8.184D-07	-2.422D-06	-2.665D-03	-3.707D-06	-5.304D-03	-9.102D-07
9	-9.070D-02	-2.709D-01	-4.318D-03	-1.008D-01	-5.008D-04	-2.117D-02
10	-2.032D-05	-1.934D-04	4.341D-01	1.553D-04	-2.652D-01	7.903D-05
11	4.595D-05	1.590D-04	-2.046D-01	-6.828D-05	1.337D-01	-3.800D-05
12	2.209D-06	6.796D-06	-7.090D-03	9.175D-08	1.134D-02	-8.927D-07
13	-5.249D-04	-1.114D-02	-2.104D-04	1.367D-02	-8.302D-06	-1.178D-01
14	3.207D-03	-6.592D-04	-3.270D-05	-3.466D-03	2.847D-05	2.352D-02

ROW \ COL	$\boxed{19}$
1	-3.916D-05
2	2.916D-05
3	5.202D-06
4	-1.854D-06
5	3.178D-04
6	8.974D-05
7	1.803D-01
8	2.451D-04
9	1.470D-02
10	-1.073D-05
11	6.639D-05
12	-2.431D-04
13	-1.769D-01
14	3.307D-02

$\boxed{}$ MODES TRUNCATED FROM DESIGN MODEL

TABLE 3-1 --CONTINUED

e) Output Weighting Matrix $\hat{Q}$ for Modal Cost Analysis

$$y_Q^2 = \eta^T \hat{Q} \eta$$

*** RETAINED MODAL OUTPUT WEIGHTING MATRIX ***

ROW \ COL	1	2	3	4	5	6	7
1	0.000D-01	0.000D-01	0.000D-01	0.000D-01	0.000D-01	0.000D-01	0.000D-01
2	0.000D-01	0.000D-01	0.000D-01	0.000D-01	0.000D-01	0.000D-01	0.000D-01
3	0.000D-01	0.000D-01	0.000D-01	0.000D-01	0.000D-01	0.000D-01	0.000D-01
4	0.000D-01	0.000D-01	0.000D-01	1.654D-06	-7.019D-10	-1.684D-09	-1.669D-10
5	0.000D-01	0.000D-01	0.000D-01	-7.019D-10	2.193D-06	1.535D-06	-1.388D-05
6	0.000D-01	0.000D-01	0.000D-01	-1.684D-09	1.535D-06	5.891D-06	-9.374D-06
7	0.000D-01	0.000D-01	0.000D-01	-1.669D-10	-1.388D-05	-9.374D-06	1.791D-04
8	0.000D-01	0.000D-01	0.000D-01	1.281D-05	-5.342D-09	-1.244D-08	-9.717D-10
9	0.000D-01	0.000D-01	0.000D-01	-4.923D-10	-3.452D-07	2.539D-06	-3.295D-06
$\boxed{10}$	0.000D-01	0.000D-01	0.000D-01	-3.820D-07	2.107D-09	-3.467D-08	2.529D-08
11	0.000D-01	0.000D-01	0.000D-01	-1.237D-06	1.122D-09	1.565D-08	-3.628D-09
12	0.000D-01	0.000D-01	0.000D-01	-3.737D-10	-7.123D-07	-1.476D-05	2.724D-06
$\boxed{13}$	0.000D-01	0.000D-01	0.000D-01	-7.363D-10	-2.598D-07	7.295D-06	-1.197D-06
14	0.000D-01	0.000D-01	0.000D-01	-4.531D-09	-6.014D-06	-3.550D-06	-3.001D-06
$\boxed{15}$	0.000D-01	0.000D-01	0.000D-01	8.791D-06	-1.360D-07	-2.157D-07	-3.335D-08
$\boxed{16}$	0.000D-01	0.000D-01	0.000D-01	3.103D-09	-3.532D-06	-3.170D-06	1.188D-05
$\boxed{17}$	0.000D-01	0.000D-01	0.000D-01	-5.642D-06	7.196D-09	7.267D-08	-1.961D-08
$\boxed{18}$	0.000D-01	0.000D-01	0.000D-01	1.666D-09	5.983D-06	3.866D-06	-8.364D-05
$\boxed{19}$	0.000D-01	0.000D-01	0.000D-01	-6.046D-10	1.010D-05	7.286D-06	-1.247D-04

ROW \ COL	8	9	$\boxed{10}$	11	12	$\boxed{13}$	14
1	0.000D-01	0.000D-01	0.000D-01	0.000D-01	0.000D-01	0.000D-01	0.000D-01
2	0.000D-01	0.000D-01	0.000D-01	0.000D-01	0.000D-01	0.000D-01	0.000D-01
3	0.000D-01	0.000D-01	0.000D-01	0.000D-01	0.000D-01	0.000D-01	0.000D-01
4	1.281D-05	-4.923D-10	-3.820D-07	-1.237D-06	-3.737D-10	-7.363D-10	-4.531D-09
5	-5.342D-09	-3.452D-07	2.107D-09	1.122D-09	-7.123D-07	-2.598D-07	-6.014D-06
6	-1.244D-08	2.539D-06	-3.467D-08	1.565D-08	-1.476D-05	7.295D-06	-3.550D-06
7	-9.717D-10	-3.295D-06	2.529D-08	-3.628D-09	2.724D-06	-1.197D-06	-3.001D-06
8	1.999D-04	4.331D-09	-7.973D-07	-5.198D-06	-1.999D-08	9.290D-09	-9.630D-09
9	4.331D-09	2.014D-06	-2.356D-08	8.746D-09	-8.075D-06	4.569D-06	3.891D-06
$\boxed{10}$	-7.973D-07	-2.356D-08	1.350D-07	3.797D-07	1.066D-07	-5.779D-08	-2.685D-08
11	-5.198D-06	8.746D-09	3.797D-07	1.115D-06	-4.195D-08	2.283D-08	5.237D-09
12	-1.999D-08	-8.075D-06	1.066D-07	-4.195D-08	4.247D-05	-2.203D-05	3.417D-07
$\boxed{13}$	9.290D-09	4.569D-06	-5.779D-08	2.283D-08	-2.203D-05	1.176D-05	3.262D-06
14	-9.630D-09	3.891D-06	-2.685D-08	5.237D-09	3.417D-07	3.262D-06	3.514D-05
$\boxed{15}$	-2.116D-07	6.772D-10	-3.498D-06	-9.548D-06	3.966D-07	-1.431D-07	6.943D-07
$\boxed{16}$	-2.909D-09	8.033D-07	-3.746D-09	-6.353D-09	3.299D-06	-2.774D-07	1.429D-05
$\boxed{17}$	-1.402D-06	4.060D-08	2.212D-06	6.061D-06	-1.951D-07	1.064D-07	1.941D-08
$\boxed{18}$	-9.229D-11	1.723D-06	-1.308D-08	-6.187D-10	-6.067D-07	4.860D-07	4.186D-06
$\boxed{19}$	1.677D-08	2.325D-06	-1.888D-08	5.420D-09	-3.412D-06	1.393D-06	-2.256D-07

ROW \ COL	$\boxed{15}$	$\boxed{16}$	$\boxed{17}$	$\boxed{18}$	$\boxed{19}$
1	0.000D-01	0.000D-01	0.000D-01	0.000D-01	0.000D-01
2	0.000D-01	0.000D-01	0.000D-01	0.000D-01	0.000D-01
3	0.000D-01	0.000D-01	0.000D-01	0.000D-01	0.000D-01
4	8.791D-06	3.103D-09	-5.642D-06	1.666D-09	-6.046D-10
5	-1.360D-07	-3.532D-06	7.196D-09	5.983D-06	1.010D-05
6	-2.157D-07	-3.170D-06	7.267D-08	3.866D-06	7.286D-06
7	-3.335D-08	1.188D-05	-1.961D-08	-8.364D-05	-1.247D-04
8	-2.116D-07	-2.909D-09	-1.402D-06	-9.229D-11	1.677D-08
9	6.772D-10	8.033D-07	4.060D-08	1.723D-06	2.325D-06
$\boxed{10}$	-3.498D-06	-3.746D-09	2.212D-06	-1.308D-08	-1.888D-08
11	-9.548D-06	-6.353D-09	6.061D-06	-6.187D-10	5.420D-09
12	3.966D-07	3.299D-06	-1.951D-07	-6.067D-07	-3.412D-06
$\boxed{13}$	-1.431D-07	-2.774D-07	1.064D-07	4.860D-07	1.393D-06
14	6.943D-07	1.429D-05	1.941D-08	4.186D-06	-2.256D-07
$\boxed{15}$	9.314D-05	3.628D-07	-5.872D-05	9.675D-08	-5.715D-08
$\boxed{16}$	3.628D-07	6.982D-06	-3.936D-08	-4.356D-06	-9.337D-06
$\boxed{17}$	-5.872D-05	-3.936D-08	3.704D-05	-5.049D-09	3.233D-08
$\boxed{18}$	9.675D-08	-4.356D-06	-5.049D-09	3.930D-05	5.806D-05
$\boxed{19}$	-5.715D-08	-9.337D-06	3.233D-08	5.806D-05	8.709D-05

$\boxed{}$ MODES TRUNCATED FROM DESIGN MODEL

TABLE 3-1 --CONCLUDED

$$\eta^T = (\eta_r^T, \eta_e^T) \;;\; d(\eta_r) = 8 \;,\; d(\eta_e) = 11 \qquad (3\text{-}9)$$

Henceforth, the notation d(.) will be used to denote vector dimension. As stated earlier, only a subset of the elastic modes will be incorporated in the design model. Thus, we can further partition η_e as

$$\eta_e^T = (\eta_{e_c}^T, \eta_{e_R}^T) \;;\; d(\eta_{e_c}) = 4 \;,\; d(\eta_{e_R}) = 7 \qquad (3\text{-}10)$$

where η_{e_c} denotes the critical elastic modes and η_{e_R} contains the residual elastic modes. The dynamical equation for the evaluation model takes the form of Equation (3-5). We leave the selection of the critical modes to be discussed in the next section.

For the design model, we assume the damping matrix $\hat{C}$ of (3-8) to be diagonal and can be written as

$$\hat{C} = \begin{bmatrix} 0 & 0 \\ 0 & 2\zeta_e\Omega_e \end{bmatrix} \qquad (3\text{-}11)$$

where ζ_e and Ω_e are both diagonal matrices containing respectively the damping ratios and natural frequencies of the modes in η_e. Furthermore, they are partitioned as

$$\begin{aligned} \zeta_e &= \mathrm{diag}\,[\zeta_c, \zeta_R] \\ \Omega_e &= \mathrm{diag}\,[\Omega_c, \Omega_R] \end{aligned} \qquad (3\text{-}12)$$

to correspond to the modal partition specified in (3-10). The input matrix B is likewise partitioned as

$$\hat{B} = \begin{bmatrix} \hat{B}_r \\ \hat{B}_{e_c} \\ \hat{B}_{e_R} \end{bmatrix} \qquad (3\text{-}13)$$

Taking the above partitioning into account, we may now write equation (3-5) as

$$\ddot{\eta}_r = \hat{B}_r u \qquad (3\text{-}14a)$$

$$\ddot{\eta}_{e_c} + 2\zeta_c \Omega_c \dot{\eta}_{e_c} + \Omega_c^2 \eta_{e_c} = \hat{B}_{e_c} u \qquad (3\text{-}14b)$$

$$\ddot{\eta}_{e_R} + 2\zeta_R \Omega_R \dot{\eta}_{e_R} + \Omega_R^2 \eta_{e_R} = \hat{B}_{e_R} u \qquad (3\text{-}14c)$$

All the elastic modes are now decoupled from one another. Only equations (3-14a) and (3-14b) are used for control design.

Finally, we assume all the physical coordinates (i.e., q_1 to q_{14} in (3-2)) are measurable.+ The measured outputs are thus related to the modal coordinates via the expression (3-3):

$$y = \tilde{E}\,\eta \qquad (3\text{-}15)$$

where $\tilde{E}$ contains the first 14 rows of the transformation matrix E in (3-3).

\+ The question of sensor selection, though a non-trivial one, will not be dealt with in this study. Suffice it to note that both inertial and proximity sensors will be required in addition to the standard attitude sensors.

Upon close examination of the data given for E in Table 3-1, one can further infer that the outputs comprise two groups

$$y = \begin{bmatrix} y_r \\ y_e \end{bmatrix}$$

where

$$y_r = (q_1 \cdots q_8)^T \quad ; \quad y_e = (q_9 \cdots\cdots q_{14})^T$$

Furthermore, the output matrix $\tilde{E}$ can be partitioned so that the output Equation (3-15) can also be written as

$$y_r = C_r \eta_r + C_{re_C} \eta_{e_C} + C_{re_R} \eta_{e_R} \qquad (3\text{-}16a)$$

$$y_e = C_{e_C} \eta_{e_C} + C_{e_R} \eta_{e_R} \qquad (3\text{-}16b)$$

We can now group together the equations for the evaluation model as follows:

(a) Spacecraft dynamics: Equations (3- 5)

(b) Outputs: Equations (3-16a)-(3-16b)

For control design, we ignore the residual modes and assume all the elastic modes to be decoupled:

(a) Spacecraft dynamics: Equations (3-14a), (3-14b)

(b) Outputs: Equations (3-16a), (3-16b) without the terms containing η_{e_R}.

3.4 Selection of Critical Modes

We return now to the question of deciding which of the elastic modes are to be included in the design model. Conventionally, modal frequency has been the chief criterion used for model selection: the idea is to include only those modes with frequencies reasonably close to the control system bandwidth. There are serious drawbacks to this approach as we shall illustrate by the following example.

Consider a system with two modes, one rigid and the other elastic, modelled by the following equations:

$$\ddot{\eta}_r = u \tag{3-17a}$$

$$\ddot{\eta}_e + 2\zeta_e\omega_e\dot{\eta}_e + \omega_e^2\eta_e = bu \tag{3-17b}$$

Here ω_e and ζ_e denote the natural frequency and damping ratio, respectively, of the elastic mode. Let the output be a linear combination of the rigid and elastic modes:

$$y = \eta_r + c\,\eta_e \tag{3-18}$$

Assume further that the same output can be differentiated to yield a rate output as

$$\dot{y} = \dot{\eta}_r + c\,\dot{\eta}_e \tag{3-19}$$

The terms bu and $c\eta_e$ in (3-17b) and (3-18) describe the control excitation of the elastic mode and its contribution to the observed output. In control jargon, they are known as 'control spillover' and 'observation spillover', respectively.

A typical design model ignoring the elastic mode would take the form

$$\ddot{\eta}_r = u \quad (3\text{-}20a)$$

$$y = \eta_r \quad (3\text{-}20b)$$

$$\dot{y} = \dot{\eta}_r \quad (3\text{-}20c)$$

Suppose the control objective is to cause the rigid mode to respond with natural frequency and damping ratio given by ω_r and ζ_r , respectively. The feedback control is then given by

$$u = -\omega_r^2 y - 2\zeta_r\omega_r \dot{y} \quad (3\text{-}21)$$

However, upon applying this control to the evaluation model (3-17) - (3-19), the closed-loop system is now described by the equations

$$\ddot{\eta}_r + 2\zeta_r\omega_r\dot{\eta}_r + \omega_r^2\eta_r = -\omega_r^2 c\,\eta_e - 2\zeta_r\omega_r c\,\dot{\eta}_e \quad (3\text{-}22a)$$

$$\ddot{\eta}_e + 2(\zeta_e\omega_e + \zeta_r\omega_r bc)\dot{\eta}_e + (\omega_e^2 + bc\,\omega_r^2)\eta_e = -\omega_r^2 b\,\eta_r - 2\zeta_r\omega_r b\,\dot{\eta}_r \quad (3\text{-}22b)$$

It can be shown that for stability, one of the necessary (but not sufficient) conditions is

$$\omega_r < -\left(\frac{\zeta_e}{\zeta_r}\right)(1 + bc)^{-1}\omega_e \quad (3\text{-}23)$$

This condition simply states that when the term (1 + bc) is negative, there is a constraint (upper bound) on the control bandwidth beyond which the closed-loop system (3-22) becomes unstable. Furthermore, this bound is not just a function of the elastic modal frequency as the conventional frequency-based modal truncation criterion seems to suggest, but is also a function of damping factors and spillover coefficients.

The rationale for the selection of the critical modes η_{ec} in (3-10) is based on the modal penalty indices defined in Reference 3. Each elastic mode is ranked according to a penalty index representing a quantitative measure of the four principal modal characteristics:

(a) Modal damping
(b) Modal frequency
(c) Modal excitation by control inputs
(d) Modal contribution to measured outputs

Note that all these four parameters are present in the condition (3-23) of our example above.

Properties (a) and (b) are defined by the structural characteristics of the spacecraft. Modal excitation is measured by the amplitude of the unit impulse response of each mode and is dependent on the actuator configuration. The modal contributions at the outputs are measured by the contribution of each mode towards a predefined performance measure. In control problems, such a measure is typically a quadratic function of the outputs:

$$Y_Q^2 = Y^T Q Y$$

Here y is related to the modal coordinates via (3-15). In general, it also depends on the sensor configuration. Following transformation, we get

$$Y_Q^2 = \eta^T \tilde{E}^T Q \tilde{E} \eta \triangleq \eta^T \hat{Q} \eta \qquad (3\text{-}24)$$

The contribution of each mode is then simply measured by the corresponding diagonal element in the weighting matrix $\hat{Q}$ (cf. Table 3-1). More will be said about the measure function (3-24) later on when we formulate the control problem.

4.0 CONTROL PROBLEM FORMULATION

As stated before, the general objective is to achieve simultaneous stationkeep and attitude control with minimal fuel expenditure. In the case of a flexible spacecraft, one must also stipulate that the above goal be accomplished with no adverse interference from the flexural modes. In other words, the dynamic spillover must not severely deteriorate the responses of the rigid modes and the critical elastic modes. In this section, we shall cast this objective in more precise mathematical terms.

4.1 Control Objective Functions

In the framework of optimal control, a quantitative measure of the operational success of stationkeep and attitude control is given by the quadratic expression

$$J_r = \int_0^{\tau} (\delta\eta_r^T Q_r \delta\eta_r)\, dt \qquad (4\text{-}1)$$

where $\delta\eta_r$ denotes the deviation of the rigid modes from a desired trajectory over the time period $(0, \tau)$. The weighting matrix Q_r determines the relative importance of the error in each mode and apart from being positive-semi-definite symmetric, is entirely arbitrary at this point.

Since the equation describing the motion of η_r is linear (cf. Equation 3-14a), there is no loss of generality in replacing $\delta\eta_r$ by η_r in (4-1). Thus, the modal cost function becomes

$$J_r = \int_0^{\tau} (\eta_r^T Q_r \eta_r)\, dt \qquad (4\text{-}2)$$

In a similar manner, we can measure the total excitation of the critical elastic modes by

$$J_e = \int_0^{\tau} (\eta_{e_c}^T Q_e \eta_{e_c})\, dt \qquad (4\text{-}3)$$

The weighting matrix Q_{ec} can again be chosen to reflect the degree of importance attached to each of the critical modes. A logical choice is the modal weighting matrix $\hat{Q}$ (3-24) used in the selection of the critical modes.

Finally, an appropriate measure of the total control energy is given by

$$J_u = \int_0^{\tau} (u^T R u)\, dt \qquad (4\text{-}4)$$

We are dealing here with two types of control inputs: gimbal torques u_g and thruster forces u_t. For gimbal torques, a cost function such as (4-4) will be adequate:

$$J_{u_g} = \int_0^{\tau} (u_g^T R_g u_g)\, dt \qquad (4\text{-}5)$$

In the case of thruster actuation, an appropriate measure of fuel consumption is the total thrust impulse.

Suppose the thrusters are fired at the discrete times τ_i where

$$0 \leq \tau_0 < \tau_1 < \cdots < \tau_{K-1} \leq \tau$$

The control thrust input may then be represented as

$$u_t(t) = \sum_{i=0}^{K-1} u_{t_i}\, \delta(t - \tau_i) \qquad (4\text{-}6)$$

where $\delta(\cdot)$ is the (Dirac) impulse function and u_{t_i} are the control impulses. The weighted total thrust impulse is therefore

$$J_{u_t} = \sum_{i=0}^{K-1} u_{t_i}^T R_t u_{t_i} \tag{4-7}$$

The total control energy is measured by summing the terms (4-5) and (4-7).

4.2 State Variable Model Representation

In order to formulate the combined stationkeep and attitude control problem in the context of multivariable optimal control we define the following state vectors:

(a) Rigid States

$$x_r^T = [\eta_{r_1} \;\; \dot{\eta}_{r_1} \;\; \cdots \;\; \eta_{r_8} \;\; \dot{\eta}_{r_8}] \tag{4-8a}$$

(b) Elastic States

(Critical) $$x_e^T = [\eta_{e_C}^T \quad \dot{\eta}_{e_C}^T] \tag{4-8b}$$

(Residual) $$x_R^T = [\eta_{e_R}^T \quad \dot{\eta}_{e_R}^T] \tag{4-8c}$$

where $d(x_r) = 16$, $d(x_e) = 8$ and $d(x_R) = 14$.

Then for the rigid states, Equation (3-14a) becomes

$$\dot{x}_r = \begin{bmatrix} A_{r_1} & & 0 \\ & \ddots & \\ 0 & & A_{r_8} \end{bmatrix} x_r + \begin{bmatrix} B_{r_1} \\ \vdots \\ B_{r_8} \end{bmatrix} u$$

$$\triangleq A_r x_r + B_r u \tag{4-9a}$$

where

$$A_{r_i} = \begin{bmatrix} 0 & 1 \\ 0 & 0 \end{bmatrix} ; \quad B_{r_i} = \begin{bmatrix} 0 \\ b^T_{r_i} \end{bmatrix} , \quad i = 1, \cdots, 8$$

The row vectors $b^T_{r_i}$ are the corresponding rows of $\hat{\mathcal{B}}_r$ in Equation (3-14a). Next, the equations for the elastic states (Equations (3-14b and c)) are written as

$$\dot{x}_e = \begin{bmatrix} 0 & I \\ -\Omega_e^2 & -2\zeta_e\Omega_e \end{bmatrix} x_e + \begin{bmatrix} 0 \\ \hat{\mathcal{B}}_{e_c} \end{bmatrix} u \triangleq A_e x_e + \mathcal{B}_e u \qquad \text{(4-9b)}$$

$$\dot{x}_R = \begin{bmatrix} 0 & I \\ -\Omega_R^2 & -2\zeta_R\Omega_R \end{bmatrix} x_R + \begin{bmatrix} 0 \\ \hat{\mathcal{B}}_{e_R} \end{bmatrix} u \triangleq A_R x_R + \mathcal{B}_R u \qquad \text{(4-9c)}$$

For ease of notation, we group the rigid states and the critical elastic states in the design model as a 'controlled' state vector:

$$x_c^T \triangleq [\, x_r^T \quad x_e^T \,] \qquad \text{(4-10)}$$

Thus, Equations (4-9a) and (4-9b) may be jointly written as

$$\dot{x}_c = \begin{bmatrix} A_r & 0 \\ 0 & A_e \end{bmatrix} x_r + \begin{bmatrix} \mathcal{B}_r \\ \mathcal{B}_e \end{bmatrix} u \triangleq A_c x_c + \mathcal{B}_c u \qquad \text{(4-11)}$$

Finally, the output equations (3-16a and b) become

$$y = \begin{bmatrix} y_r \\ y_e \end{bmatrix} = \begin{bmatrix} \mathbb{C}_r & \mathbb{C}_{re} \\ 0 & \mathbb{C}_e \end{bmatrix} \begin{bmatrix} x_r \\ x_e \end{bmatrix} + \begin{bmatrix} \mathbb{C}_{re_R} \\ \mathbb{C}_{e_R} \end{bmatrix} x_R \qquad \text{(4-12)}$$

$$\triangleq C_c x_c + C_R x_R$$

Here the coefficient matrices are defined as follows:

$$\mathbb{C}_r = [\, c_{r_1} \;\; 0 \;\; c_{r_2} \;\; 0 \;\; \cdots \;\; c_{r_8} \;\; 0 \,]$$

$$\mathbb{C}_{re} = [\, C_{re_c} \;\; 0 \,] \quad ; \qquad \mathbb{C}_{re_R} = [\, C_{re_R} \;\; 0 \,] \tag{4-12a}$$

$$\mathbb{C}_e = [\, C_{e_c} \;\; 0 \,] \quad ; \qquad \mathbb{C}_{e_R} = [\, C_{e_R} \;\; 0 \,]$$

The vectors c_{r_i} are the corresponding columns of the matrix C_r in (3-16a).

In terms of the state variables just defined, the cost functions (4-2) and (4-3) can be expressed jointly as

$$J_c = \int_0^{\tau} (x_c^T Q_c x_c)\, dt \tag{4-13}$$

where the weighting matrix Q_c is derived directly from the modal weighting matrices Q_r and Q_{e_c}. Note that since x_c contains both (η_r , η_{e_c}) and ($\dot{\eta}_r$, $\dot{\eta}_{e_c}$), rate penalties may easily be incorporated into the cost function.

4.3 Statement of Control Problem

The combined stationkeep and attitude control problem can now be stated in the framework of optimal control as follows:

Given the system model

$$\dot{x}_c = A_c x_c + B_c u \tag{4-11}$$

$$\dot{x}_R = A_R x_R + B_R u \tag{4-9c}$$

$$y = C_c x_c + C_R x_R \tag{4-12}$$

where the control input u is partitioned as

$$u^T = (u_g^T \quad u_t^T)$$

Find the gimbal torque input u_g and the thruster impulse sequence

$$u_t = \sum_{i=0}^{K-1} u_{t_i} \, \delta(t-\tau_i) \qquad (4\text{-}6)$$

with

$$0 \leq \tau_0 < \tau_1 < \cdots < \tau_{K-1} \leq \tau$$

so as to minimize the cost function

$$J = \int_0^{\tau} (x_c^T Q_c x_c + u_g^T R_g u_g) dt + \sum_{i=0}^{K-1} u_{t_i}^T R_t u_{t_i} + x_c^T(\tau) Q_{c_K} x_c(\tau) \qquad (4\text{-}14)$$

The last term is a penalty function of the terminal condition of x_c. Furthermore, to be admissible, the control inputs must be functions only of the oututs in y.

The control problem just stated is a variation of the standard linear optimal regulator problem (see, e.g., Reference 6), the variation being the presence of both discrete and continuous-time variables in the cost function (4-14). The general solution is given in the linear feedback form as

$$u = F \hat{x}_c \qquad (4\text{-}15)$$

where $\hat{x}_c$ denotes an estimate of the controlled variables x_c obtained from the outputs y. Figure 4-1 depicts the overall configuration of the modal compensator for design and evaluation.

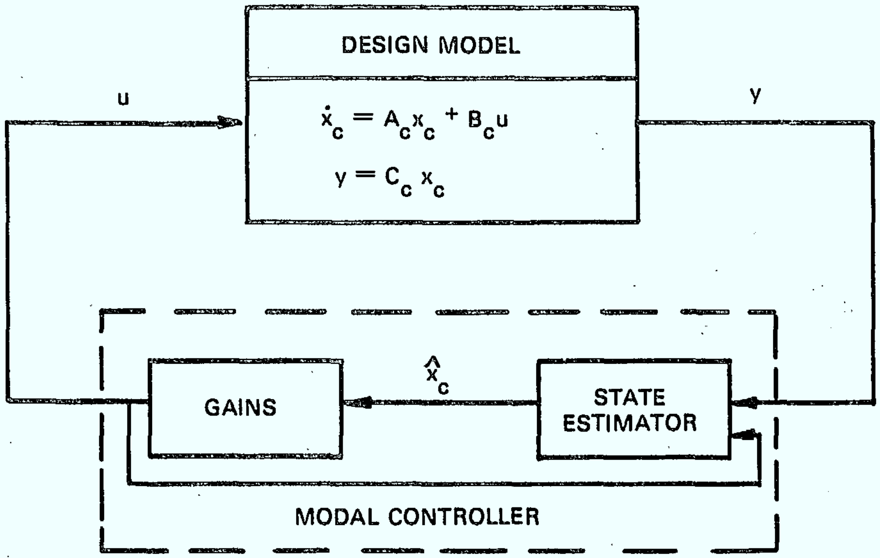

A) DESIGN

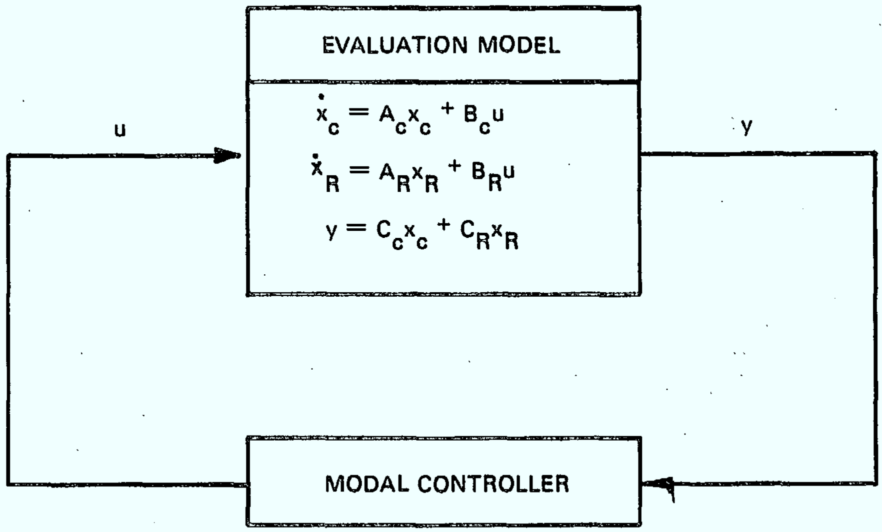

B) EVALUATION

FIGURE 4-1 MODAL CONTROL DESIGN AND EVALUATION

The rest of this report will be devoted to separate investigations of the controller and observer designs. In particular, we shall discuss such topics as:

(a) Controllability and observability conditions

(b) Controller design with (control) spillover compensation

(c) Observer design with (observation) spillover compensation

(d) Full-order versus reduced-order observer.

5.0 CONTROLLER DESIGN

5.1 Controllability Conditions

One of the first requirements for control design is that the system model must be completely controllable. In a qualitative sense, this means that all the controlled variables can be independently driven to arbitrary values with appropriately designed control inputs. In the case of linear optimal control, controllability also ensures the stability of the closed-loop system.

For linear systems such as Equation (4-11), the condition for controllability is well documented in the literature. Essentially, the so-called controllability matrix

$$\mathcal{C} \triangleq \left[B_c \;\; A_c B_c \;\; A_c^2 B_c \;\; \cdots \;\; A_c^{N-1} B_c \right] \qquad (5\text{-}1)$$

must have rank N, the number of controlled variables in x_c. In the case of flexible spacecraft, this condition can be simplified considerably once it is realized that Equation (4-11) in fact originates from the second-order modal equations (3-14). In terms of the parameters of the modal equations, the controllability conditions are as follows (see Reference 7):

(a) $\text{rank}\ \hat{B}_r = d(\eta_r) = 8$ (5-2a)

(b) When all the elastic modal frequencies are distinct, each row of $\hat{B}_{e_c}$ must contain at least one non-zero element. (5-2b)

It is interesting to note that Condition (5-2a) also imposes a lower bound on the number of actuators required, viz

$$d(u) \geq d(\eta_r) \qquad (5\text{-}2c)$$

From the data listed in Table 3-1, it is seen that (5-2b) is easily satisfied. However, the matrix $\hat{B}_r$ has at most a rank of 7, since the third row is identically zero. This is due to the obvious fact that the given thruster configuration(Figure 2-2) is unable to cause any motion in the radial (i.e., altitudinal) direction of the orbit. However, since stationkeep normally does not involve adjustment of the orbital radius, there is no need to include the radial motion equation in the system model. Thus, following the omission of η_{r_3} and $\dot{\eta}_{r_3}$ from the controlled variables x_c, the system represented by Equation (4-11) is now completely controllable.

5.2 Optimal Feedback Control Algorithm

We shall first obtain the standard solution to the optimal control problem posed in Section 4.3. The control algorithm will be modified later on to incorporate spillover compensation, a major feature in the control of flexible spacecraft.

Let us first collect the system equations from Section 4.0:

$$\dot{x}_c = A_c x_c + B_c u = A_c x_c + B_{c_g} u_g + B_{c_t} u_t \qquad (4\text{-}11)$$

$$\left(\dot{x}_R = A_R x_R + B_R u = A_R x_R + B_{R_g} u_g + B_{R_t} u_t\right) \qquad (4\text{-}9c)$$

$$y = C_c x_c \;\left(+ C_R x_R\right) \qquad (4\text{-}12)$$

where

$$u^T \triangleq \left(u_g^T \quad u_t^T\right)$$

and

$$d(x_c) = 22\,,\quad d(x_R) = 14\,,\quad d(u_g) = 2\,,\quad d(u_t) = 8$$

The terms in the parentheses are omitted from the design model.

We make the following assumptions about the control input u . The thruster inputs are defined by the impulse sequence

$$u_t(t) = \sum_{i=0}^{K-1} u_{t_i} \delta(t-\tau_i) \qquad (4\text{-}6)$$

The gimbal torques are taken to be constant over each sampling interval so that

$$u_g(t) = u_{g_i} \quad , \quad \tau_i \leq t < \tau_{i+1} \; , \; i=0,\cdots,K-1 \qquad (5\text{-}3)$$

Furthermore, we assume the sampling interval to be constant with

$$0 = \tau_0 < \tau_1 \cdots\cdots < \tau_{K-1} < \tau_K = \tau$$

and

$$\tau_{i+1} - \tau_i = \Delta\tau \quad , \quad i = 0, \cdots, K-1$$

The design objective is to find the control sequences

$$\{u_{t_i}\} \; , \; \{u_{g_i}\}$$

which minimize a cost function given by

$$J = \int_0^{\tau} (x_c^T Q_c x_c + u_g^T R_g u_g) \, dt + \sum_{i=0}^{K-1} u_{t_i}^T R_t u_{t_i} + x_c^T(\tau) Q_{c_K} x_c(\tau) \qquad (4\text{-}14)$$

All the weighting matrices here are taken to be symmetric and positive semi-definite; in addition, the matrices R_g and R_t are positive definite.

The optimal control solution can be obtained using a classical dynamic programming technique (Reference 8). We shall quote only the result here; the interested reader is referred to Appendix A for details. First define the following matrices (cf. (A-7)):

$$\left.\begin{aligned}
\bar{Q} &\triangleq \int_0^{\Delta\tau} (e^{A_c t})^T Q_c (e^{A_c t})\, dt \\
B_u(t) &\triangleq \left[\int_0^t e^{-A_c s} ds\, B_{c_g} \qquad B_{c_t} \right] \\
\bar{P} &\triangleq \int_0^{\Delta\tau} (e^{A_c t})^T Q_c (e^{A_c t})\, B_u(t)\, dt \\
\bar{R} &\triangleq \mathrm{diag}\left[R_g \Delta\tau ,\ R_t \right] + \int_0^{\Delta\tau} (e^{A_c t} B_u(t))^T Q_c (e^{A_c t} B_u(t))\, dt \\
\bar{A}_c &\triangleq e^{A_c \Delta\tau} \quad ; \quad \bar{B}_c \triangleq \bar{A}_c B_u(\Delta\tau)
\end{aligned}\right\} \quad (5\text{-}4)$$

Then one can show that the cost function (4-14) is discretized as

$$J = \sum_{k=0}^{K-1} \left(x_{c_k}^T \bar{Q}\, x_{c_k} + 2 x_{c_k}^T \bar{P}\, u_k + u_k^T \bar{R}\, u_k \right) + x_{c_K}^T Q_{c_K} x_{c_K} \qquad (5\text{-}5)$$

where the control vector is defined by

$$u_k^T \triangleq \left[u_{g_k}^T \quad u_{t_k}^T \right]$$

Here and below, the subscript k will be used to denote the value of a variable at the sample time τ_k .

The optimal control sequence is given by

$$u_k = F_k\, x_{c_k} \qquad (5\text{-}6)$$

in which the feedback gain matrix is computed from the following recursive equations (solved backwards):

$$\left.\begin{aligned}F_k &= -\left[\bar{R} + \bar{B}_c^T Q_{k+1} \bar{B}_c\right]^{-1} \left[\bar{P} + \bar{A}_c^T Q_{k+1} \bar{B}_c\right]^T \\ Q_k &= \bar{Q} + \bar{A}_c^T Q_{k+1} \bar{A}_c + \left[\bar{P} + \bar{A}_c^T Q_{k+1} \bar{B}_c\right] F_k \\ Q_K &= Q_{c_K}\end{aligned}\right\} \quad (5\text{-}7)$$

The value of the cost function (5-5) with this control law is given by

$$J_{optimal} = x_{c_0}^T Q_0 \, x_{c_0} \quad (5\text{-}8)$$

Although the control algorithm (5-6), (5-7) can be conveniently implemented on a digital computer, it is still too complicated to be practical, since on-line computation will be required at each sampling interval. Fortunately, there is a standard control theorem which says that if the system (4-11) is completely controllable and 'reconstructible'+, then the matrix sequence $\{Q_k\}$ will converge (as k approaches zero) to the same constant steady state solution Q from any terminal condition Q_K and for sufficiently large K. The steady state control law thus has the simple form

$$u_k = \bar{F} \, x_{c_k} \quad (5\text{-}9)$$

\+ We shall not be too concerned with the latter concept here; suffice it to say that the system is reconstructible if the weighting matrix Q_c is diagonal and has a positive value associated with each of the position variables in x_c .

where the constant feedback gain matrix is given by

$$\bar{F} = -\left[\bar{R} + \bar{B}_c^T Q \bar{B}_c\right]^{-1}\left[\bar{P} + \bar{A}_c^T Q \bar{B}_c\right] \qquad (5\text{-}10)$$

The optimal cost is given by

$$J_{optimal} = x_{c_0}^T Q x_{c_0}$$

Thus, to obtain the constant feedback gain, it is only necessary to calculate the steady state solution of the recursive equation (5-7) for a sufficiently large value of K.

Finally, and most important of all, the same theorem also asserts that the closed-loop system with (5-9) applied to (4-11) will be asymptotically stable. This stability property will be explored further in the next section.

5.3 Stability Analysis

Following the approach taken in Appendix A, we can discretize the system equations (4-11), (4-9c) and (4-12) as

$$x_{c_{k+1}} = \bar{A}_c x_{c_k} + \bar{B}_c u_k \qquad (5\text{-}11a)$$

$$x_{R_{k+1}} = \bar{A}_R x_{R_k} + \bar{B}_R u_k \qquad (5\text{-}11b)$$

$$y_k = C_c x_{c_k} + C_R x_{R_k} \qquad (5\text{-}11c)$$

where

$$\bar{A}_c \triangleq e^{A_c \Delta\tau} \; ; \; \bar{B}_c \triangleq e^{A_c \Delta\tau}\left[\int_0^{\Delta\tau} e^{-A_c s} ds \, B_{c_g} \quad B_{c_t}\right]$$

$$\bar{A}_R \triangleq e^{A_R \Delta\tau} \; ; \; \bar{B}_R \triangleq e^{A_R \Delta\tau}\left[\int_0^{\Delta\tau} e^{-A_R s} ds \, B_{R_g} \quad B_{R_t}\right]$$

With the steady state control law (5-9) in place, the closed-loop system dynamics are described by the equation

$$\begin{bmatrix} x_{c_{k+1}} \\ x_{R_{k+1}} \end{bmatrix} = \begin{bmatrix} \bar{A}_c + \bar{B}_c \bar{F} & 0 \\ \bar{B}_R \bar{F} & \bar{A}_R \end{bmatrix} \begin{bmatrix} x_{c_k} \\ x_{R_k} \end{bmatrix} \qquad (5\text{-}12)$$

As pointed out earlier, controllability ensures that Equation (5-11a) remains stable in closed loop; that is, all the eigenvalues of the matrix ($\bar{A}_c + \bar{B}_c \bar{F}$) have magnitudes less than unity. The residual states x_R are inherently stable since they represent elastic modes of the spacecraft. Hence, the closed-loop system (5-12) remains dynamically stable despite the presence of the control spillover term $\bar{B}_R \bar{F}$.

The above stability analysis hinges on the assumption that all the controlled states x_c are available for feedback, which is almost never the case. In practice, only estimates of x_c are at best available from observing the outputs, which, from (5-11c), are clearly influenced by both the residual and the controlled state variables. Hence, even though the control spillover by itself will not destabilize the closed-loop system, it is advisable to avoid exciting the residual modes too much if only to preserve the integrity of the state estimates.

5.4 Optimal Control with Spillover Compensation

Many ways have been suggested in the literature for the removal or suppression of control spillover. Within the framework of optimal control, an obvious approach (cf. Reference 9) is to include an extra term in the cost function which directly penalizes the control spillover. To do this, it is only necessary to replace the control weighting matrices in the cost function of (4-14) by the following:

$$\bar{R}_g = R_g + B_{R_g}^T W_g B_{R_g}$$
$$\bar{R}_t = R_t + B_{R_t}^T W_t B_{R_t} \tag{5-13}$$

Here the positive-definite matrices W_g and W_t are used to penalize the control inputs causing the spillover:

$$B_R u = B_{R_g} u_g + B_{R_t} u_t$$

The same control algorithm of Section 5.2 now applies.

6.0 OBSERVER DESIGN

6.1 Observability Conditions

Consider the system model given by the equations

$$\dot{x}_c = A_c x_c + B_c u \tag{4-11}$$

$$\dot{x}_R = A_R x_R + B_R u \tag{4-9c}$$

$$y = C_c x_c + C_R x_R \tag{4-12}$$

A dual property to controllability is the ability to reconstruct the state variables from the observed outputs. In this case, we are concerned only with the observability of the controlled state vector x_c.

The classical condition for observability is that the so-called observability matrix

$$\mathcal{O} \triangleq \left[C_c^T \quad A_c^T C_c^T \quad A_c^{T2} C_c^T \quad \cdots \quad (A_c^T)^{N-1} C_c^T \right] \tag{6-1}$$

must have a rank equal to the number of variables in x_c (i.e., N). Duality to controllability is evident when (6-1) is compared to the controllability matrix in (5-1).

In the case of flexible spacecraft, this observability condition can be expressed in terms of the parameters of the second order equations (3-14) and (3-16) (cf. Reference 7):

(a) $\text{rank } C_r = d(\eta_r) = 7$ + (6-2a)

(b) When all the modal frequencies are distinct each column of

$$\begin{bmatrix} C_{re_c} \\ C_{e_c} \end{bmatrix} \tag{6-2b}$$

+ Henceforth, we shall omit the radial translation mode η_{r_3} from η_r.

must contain at least one non-zero element.

From the data provided in Table 3-1, we note that (6-2b) is readily satisfied. Furthermore, C_r is a triangular matrix with full rank. Therefore, we conclude that all the variables in x_e are observable from the outputs in y.

As a corollary, a necessary condition to (6-2a) is that (cf. (3-16a))

$$d(y_r) \geq d(\eta_r) \tag{6-3}$$

In other words, there should be at least as many independent measurements of the rigid states as there are of the rigid modes.

6.2 Full-Order Versus Reduced-Order Observers

Before we proceed with design, the issue of the size of the observer must be resolved. Classical observer theory asserts that given a completely observable system, such as (4-11) and (4-12), the observer may be of the same order as the system (i.e., $d(x_e)$) or of a lower order given by ($d(x_e) - d(y)$). This is because part of the information needed for state reconstruction is already present in the output y.

Reduced-order observers have the obvious advantage of being less complex in comparison to full-order observers. As illustration, we have here

$$d(x_c) = 2\,[\,d(\eta_r) + d(\eta_{e_c})\,]$$
$$= 14 + 8 = 22$$

$$d(y) = d(y_r) + d(y_e)$$
$$= 7 + 6 = 13$$

Thus, a reduced-order observer contains only 9 states, whereas a full-order observer would require 22 state variables.

The major drawback of reduced-order observers is that when the observer is imbedded in a control loop, the dynamics of the closed-loop system could be severely altered by the presence of spillover from the unmodelled modes. A trade-off between observer complexity and performance sensitivity is fully discussed in Appendix B. The recommendation there is that in the case of flexible spacecraft, it is preferable to use full-order observers augmented with appropriate spillover compensation schemes.

6.3 Decoupled Observer Design

In the case of flexible spacecraft, the configuration of the full-order observer can be simplified considerably by taking advantage of the decoupled modal characteristics as demonstrated by the modal equations (3-14) and (3-16). In particular, the elastic modes are completely decoupled from the rigid modes both in the dynamical equations (3-14) and in the outputs (3-16). This is a clear indication that these modes may be observed independently of the rigid modes, provided, of course, that appropriate observability conditions are satisfied.

As in Section 4.2, we separate the rigid and the elastic state variables in the model (cf. (4-9))

$$\dot{x}_r = A_r x_r + B_r u \tag{6-4a}$$

$$\dot{x}_e = A_e x_e + B_e u \tag{6-4b}$$

Similarly, the outputs are given by

$$y_r = \mathbb{C}_r x_r + \mathbb{C}_{re} x_e + C_{re_R} \eta_{e_R} \tag{6-5a}$$

$$y_e = \mathbb{C}_e x_e + C_{e_R} \eta_{e_R} \tag{6-5b}$$

where all the matrices have been defined in (4-12a).

Consider first the elastic state equations (6-4b) and (6-5b). If all the elastic state variables in x_e are to be observable from y_e alone, then a condition similar to (6-2b) must be satisfied; viz, there must be no zero column in C_{ee}, the output matrix imbedded in $\mathbb{C}_e$ (cf. (4-12a)). That this is indeed the case is evident from the data provided in Table 3-1.

A full-order observer for x_e is given by

$$\dot{\hat{x}}_e = (A_e - K_e \mathbb{C}_e)\hat{x}_e + B_e u + K_e y_e \tag{6-6}$$

The estimation error is described by the equations

$$\varepsilon_e \triangleq \hat{x}_e - x_e$$

$$\dot{\varepsilon}_e = (A_e - K_e \mathbb{C}_e)\varepsilon_e + K_e C_{e_R} \eta_{e_R} \tag{6-7}$$

Consider next the rigid state equations (6-4a) and (6-5a). Satisfaction of the condition (6-2a) guarantees the observability of x_r from y_r alone. An observer for the rigid state vector is thus given by

$$\dot{\hat{x}}_r = (A_r - K_r \mathbb{C}_r)x_r + B_r u + K_r(y_r - \mathbb{C}_{re}\hat{x}_e) \qquad (6\text{-}8)$$

The estimation error dynamics are described by the equations

$$\varepsilon_r \triangleq \hat{x}_r - x_r$$

$$\dot{\varepsilon}_r = (A_r - K_r \mathbb{C}_r)\varepsilon_r - K_r \mathbb{C}_{re}\varepsilon_e + K_r C_{re_R}\eta_{e_R} \qquad (6\text{-}9)$$

Further simplification of the rigid state observer (6-8) is possible if one recognizes the fact (cf. Table 3-1) that the output matrix C_r in $\mathbb{C}_r$ is triangular with full rank. Since A_r is block diagonal (cf. (4-9a)), the gain K_r can also be chosen to be block diagonal without affecting the stability properties of ($A_r - K_r \mathbb{C}_r$). Thus, the full-order observer (6-8) may be further decoupled into a bank of second-order observers, one for each of the rigid modes.

Combining the error equations (6-7) and (6-9), we get

$$\begin{bmatrix} \dot{\varepsilon}_r \\ \dot{\varepsilon}_e \end{bmatrix} = \begin{bmatrix} (A_r - K_r\mathbb{C}_r) & -K_r\mathbb{C}_{re} \\ 0 & (A_e - K_e\mathbb{C}_e) \end{bmatrix} \begin{bmatrix} \varepsilon_r \\ \varepsilon_e \end{bmatrix} + \begin{bmatrix} K_r C_{re_R} \\ K_e C_{e_R} \end{bmatrix} \eta_{e_R} \qquad (6\text{-}10)$$

Observability implies that the gain matrices K_r and K_e may be separately chosen to stabilize the matrices ($A_r - K_r \mathbb{C}_r$) and

($A_e - K_e C_e$), respectively. As a consequence, the estimation errors will be bounded provided the observation spillover terms from η_{eR} are bounded. The configuration for the decoupled observers is depicted in Figure 6-1.

6.4 Observer with Spillover Compensation

As demonstrated in Appendix B, it is entirely possible for the spillover terms to destabilize the system once the observer is included in the control loop. In this section, we shall seek ways of compensating for the spillover effects.

It is apparent from (6-10) that the observer in fact also acts as a low-pass filter on the residual modes; the filter dynamics being determined by the observer gains. When all the residual modes in η_{eR} lie well outside of the observer bandwidth, the spillover effects should be minimal. Hence, an obvious approach is to constrain the observer bandwidth to be well below the lowest frequency of the residual modes. Unfortunately, this also restricts the response speed of the observer to a rate which may not be acceptable for control purposes. In this case, active suppression of the spillover terms may be necessary.

A method of active spillover compensation is presented in Appendix C. We shall now apply this technique to the decoupled observers. Consider first the elastic modal observer ((6-6) and (6-7)). From Appendix C, the design conditions for the gain K_e are

(a) $K_e C_{eR_i} = 0 \quad , i = 1, \cdots, p$ (6-11a)

(b) $(A_e - K_e C_e)$ is stable with arbitrary pole allocation. (6-11b)

Here we have chosen to suppress spillover from a subset of the residual modes in η_{eR}. The number of suppressed modes (p) must be less than the number of elastic modal measurements in (6-5b); viz,

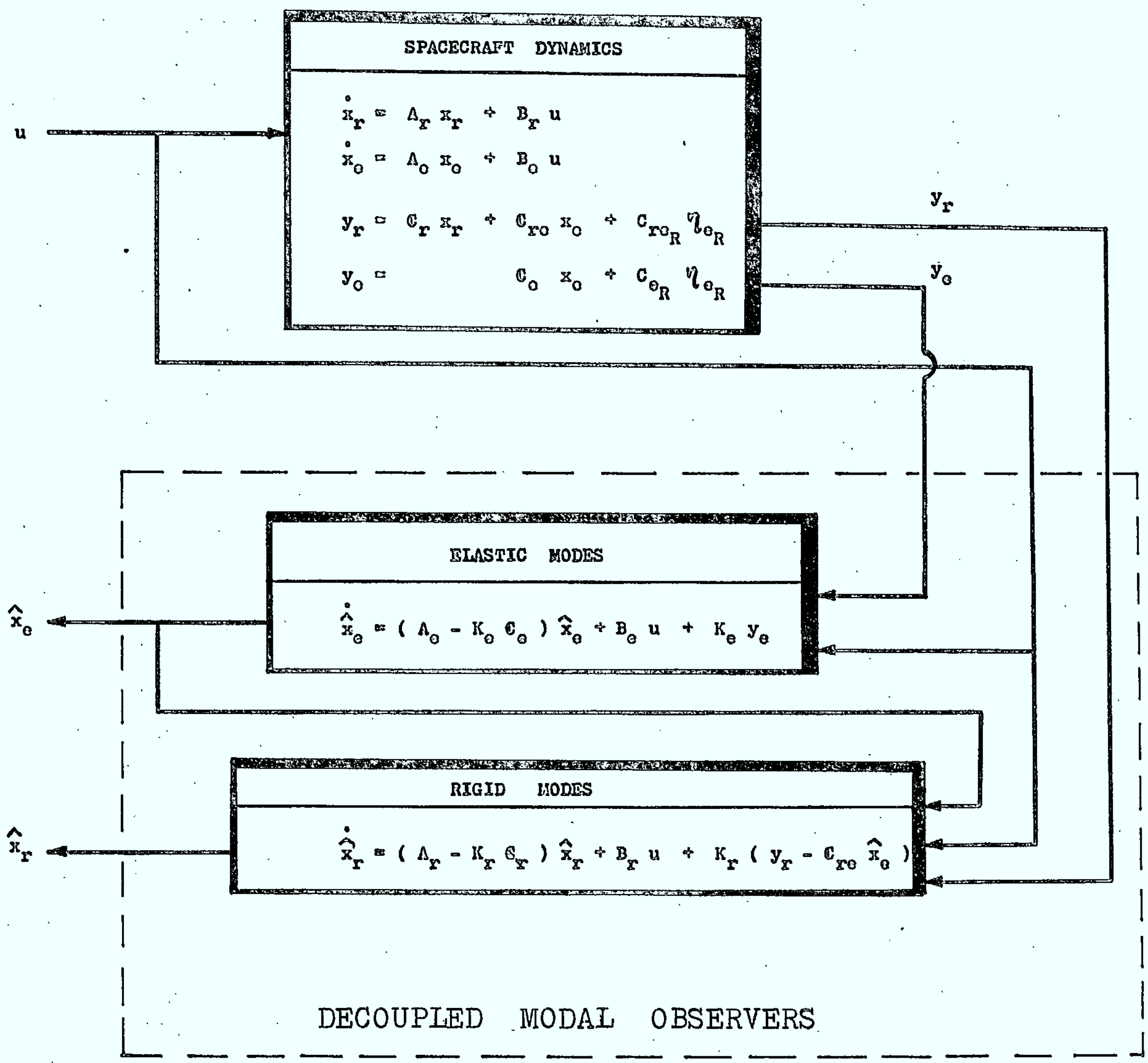

FIGURE 6-1 DECOUPLED OBSERVER CONFIGURATION

$$p < d(y_e) \tag{6-12}$$

Assume all the columns

$$\{ C_{eR_i} \,,\ i=1,\cdots,p \}$$

are linearly independent. Then a matrix $\bar{K}_e$ is bound to exist such that

$$\bar{K}_e C_{eR_i} = 0 \quad , \ i=1,\cdots,p \tag{6-13}$$

Here $\bar{K}_e$ is a $(d(y_e)-p) \times d(y_e)$ matrix with full rank. Furthermore, any matrix K_e satisfying (6-11a) must be of the form

$$K_e = \Lambda \bar{K}_e \tag{6-14}$$

Hence, the problem of finding K_e to satisfy (6-11) is reduced to that of finding Λ to stabilize ($A_e - \Lambda \bar{K}_e \mathbb{C}_e$). This is possible if and only if the pair ($\bar{K}_e \mathbb{C}_e$, A_e) is observable. Using an approach similar to Appendix C, it can be shown that ($\bar{K}_e \mathbb{C}_e$, A_e) is observable if and only if the matrix product $\bar{K}_e C_{e_e}$ contains no zero column.

We can now summarize the design algorithm for K_e as follows:

(a) Select up to ($d(y_e) - 1$) modes from η_{eR} whose frequencies fall within the desired bandwidth of the observer.

(b) Ascertain that the corresponding columns in C_{eR} are linearly independent.

(c) Solve for $\bar{K}_e$ such that

$$\bar{K}_e C_{e R_i} = 0 \ , \quad i = 1, \cdots, p$$

(Standard procedures can be found in any textbook on Linear Algebra).

(d) Check that $\bar{K}_e C_{e_C}$ contains no zero column;* if not, return to (a) for a new selection of suppressed modes.

(e) Find Λ to set the eigenvalues of ($A_e - \Lambda \bar{K}_e \mathbb{C}_e$) to match the desired observer bandwidth.

(f) Calculate the observer gain from

$$K_e = \Lambda \bar{K}_e$$

We consider next the rigid state observer (6-8). It is now required to choose the gain K_r so that

(a) $K_r C_{re R_i} = 0 \ , \quad i = 1, \cdots, p$ (6-15a)

(b) ($A_r - K_r \mathbb{C}_r$) is stable with arbitrary pole allocation. (6-15b)

Here, the columns of C_{re_R} must correspond to the columns of C_{e_R} selected earlier in (6-11a).

Suppose for the moment that a full rank matrix $\bar{K}_r$ can be found such that

$$\bar{K}_r C_{re R_i} = 0 \ , \quad i = 1, \cdots, p$$

Note that for $\bar{K}_r$ to exist, it is necessary that

$$p < d(y_r)$$

---

* Typically, this condition holds generically (i.e., for almost any parameter set).

Since we have assumed C_r to have full rank, this is equivalent to

$$p < d(\eta_r) \tag{6-16}$$

As before, we argue that the conditions in (6-15) are now reduced to choosing Λ to stabilize the matrix ($A_r - \Lambda \bar{K}_r C_r$). For this, the matrix product $\bar{K}_r C_r$ must have a rank of $d(\eta_r)$. However, $\bar{K}_r C_r$ only has ($d(\eta_r) - p$) rows and thus obviously cannot have a rank of $d(\eta_r)$. This shows that the pair ($\bar{K}_r C_r$, A_r) is not completely observable. As a consequence, we conclude that the same residual modes suppressed in the elastic modal observer cannot be entirely suppressed in the rigid modal observer. In order to do so, one may use the fully coupled observer configuration as demonstrated in Appendix C.

7.0 PRACTICAL CONSIDERATIONS

With the observer discussion of Section 6.0, we have essentially completed the theoretical development of the compensator design. This section deals with some of the practical aspects pertaining to either the implementation or the limitations of the design accomplished so far.

7.1 Implementation of Negative Control Thrusts

With the thruster configuration given in Figure 2-2, negative control thrusts are inadmissible since the thrusters would be firing directly into the spacecraft. To overcome this deficiency, each negative thrust demand must be replaced by a set of positive thrust commands for the remaining thrusters so as to generate the equivalent amount of control torque on the spacecraft. Furthermore, this must be accomplished with minimal expenditure of additional fuel.

The control torque vector generated by the thrusters are given by

$$\hat{B}_t u_t = \sum_{i=1}^{8} b_{t_i} u_{t_i} \tag{7-1}$$

where b_{t_i} are the corresponding columns in the thruster input distribution matrix of (3-13); their numerical values are listed in Table 3-1. From the thruster configuration of Figure 2-2, it is clear that the thrusters at the reflector hub are aligned in a diagonally opposite manner so that

$$u_{t_5} = -u_{t_7} \tag{7-2a}$$

$$u_{t_6} = -u_{t_8} \tag{7-2b}$$

In terms of the data for the input distribution matrix of (7-1), this simply means that

$$b_{t_5} = -b_{t_7} \tag{7-3a}$$

$$b_{t_6} = -b_{t_8} \tag{7-3b}$$

Hence, negative thrust commands for any of the thrusters on the reflector hub may be replaced by positive thrust commands of the same magnitudes for the diagonally opposite thruster.

In the case of the thrusters on the main bus, one observes from the data in Table 3-1 that

$$-b_{t_i} = \sum_{\substack{j=1 \\ j \neq i}}^{4} b_{t_j} \quad , \quad i=1,\cdots,4 \tag{7-4}$$

This means a negative thrust applied at any of the thrusters on the bus will produce the equivalent control torque of a positive thrust of the same magnitude applied simultaneously at each of the remaining thrusters on the bus.

The logic for implementing negative control thrusts can thus be summarized as follows:

For thrusters on the main bus: $(i=1,\cdots,4)$

$$u_{t_i} < 0 \iff \begin{array}{l} u_{t_j} = |u_{t_i}| \quad , \quad j \neq i \\ u_{t_i} = 0 \end{array} \tag{7-5a}$$

For thrusters at the reflector hub: $(i=5,\cdots,8)$

$$\left.\begin{aligned} u_{t_5} < 0 &\iff u_{t_7} = |u_{t_5}|, \quad u_{t_5} = 0 \\ u_{t_6} < 0 &\iff u_{t_8} = |u_{t_6}|, \quad u_{t_6} = 0 \\ u_{t_7} < 0 &\iff u_{t_5} = |u_{t_7}|, \quad u_{t_7} = 0 \\ u_{t_8} < 0 &\iff u_{t_6} = |u_{t_8}|, \quad u_{t_8} = 0 \end{aligned}\right\} \qquad (7\text{-}5b)$$

We shall next show that the above algorithm is in fact a minimal-fuel implementation of negative control thrusts. In the case of the thrusters at the hub (7-5b), it is clear that the fuel consumption remains unchanged. However, with the thrusters at the bus (7-5a), there is a three-fold increase in fuel consumption. We shall show that this increase is indeed the minimum required.

Suppose a negative thrust demand occurs at thruster i at the bus. The problem is to find the positive coefficients α_j for the expression

$$b_{t_i} u_{t_i} = \sum_{j=1}^{4} b_{t_j} \alpha_j \qquad (7\text{-}6)$$

where each α_j represents the thrust required of the corresponding thruster at the bus so that the total control torque is the same as that produced by the negative thrust alone. Substitution of (7-4) into (7-6) yields

$$\sum_{\substack{j=1 \\ j \neq i}}^{4} b_{t_j} (\alpha_j - \alpha_i + u_{t_i}) = 0 \qquad (7\text{-}7)$$

Provided the vectors $\{ b_{t_j} , j \neq i \}$ are linearly independent for each i (cf. Table 3-1), we get

$$\alpha_j = \alpha_i - u_{t_i} , \quad j \neq i \qquad (7\text{-}8)$$

Clearly, there are an infinite number of solutions to this equation for each u_{t_i}. Also, when u_{t_i} is negative, there always exist positive values of α_j that satisfy (7-8). But the solution that minimizes the total fuel requirement is given by

$$\begin{aligned} \alpha_i &= 0 \\ \alpha_j &= |u_{t_i}|, \quad j \neq i \end{aligned} \qquad (7\text{-}9)$$

This completes the proof of our claim.

7.2 Parameter Uncertainties

Uncertainties in the design parameters arise from various sources ranging from model infidelity to thruster misbehaviour. The following are some of the major causes.

(a) Modal Data Uncertainties

For spacecraft of modest dimensions, such as Hermes, it has been possible to verify the modal data by ground testing prior to finalization of the controller parameters. However, due to the sizes of third-generation spacecraft, it is unlikely that ground-based testing facilities will be available. Experience in the past has revealed that errors of up to an order of magnitude are possible between design and flight data (see Reference 11). This is especially a problem for some parameters, such as damping factor, which are based at best on 'guesstimation'. Although the situation can be ameliorated to a certain extent by post-launch modification of the control software, a healthy stability margin must be built into the compensator design.

(b) Unmodelled Dynamics

Unmodelled sensor and actuator dynamics could present stability problems if their transfer lags significantly affect the bandwidth of the closed-loop system. For instance, experience (References 12 and 13) has shown that the performance of the observer is particularly sensitive to variations in thruster dynamics and unmodelled external disturbances. In addition, sensor and actuator noises also cause performance deterioration although closed-loop stability will not likely be affected.

Inclusion of sensor or actuator dynamics in the compensator model will no doubt increase the design complexity but may be unavoidable in certain cases. External disturbances may be compensated in a feedforward manner provided reliable estimates are available. Finally, noise filters are admissible in the control loop as long as the compensator dynamics are not severely disturbed. Only experimentation with hardware complemented by extensive computer simulation can provide sufficient reassurance of the robustness of the compensator design.

(c) In-Flight Parameter Variation

There are many causes for the variation of control system parameters during the lifetime of a spacecraft; the major ones are fuel depletion, structural deformation, material deterioration and failure of deployment mechanisms. This could present a serious problem in large spacecraft with distributed masses and flexible structures where, for instance, any movement of the centre-of-mass can greatly affect the control and disturbance torques.

With the growing use of on-board microprocessors, re-programming of the control software during flight may be considered as an operational option provided the parametric variations can be successfully identified and monitored on-line. Nevertheless, it is advisable that such measures should be attempted only if supplemented by thorough verification procedures on the ground. The ability to transfer control into a reliable back-up mode is essential.

7.3 Spillover from Unknown Modes

Since flexible structures are described by partial differential equations, there are, in principle, an infinite number of vibration modes. The model hierarchy we have considered (Figure 3-3) originated from a finite-dimensional model with a total of 73 coordinates. Following truncation, only eight rigid modes and 11 elastic modes were retained in the evaluation model. Of these elastic modes, only four were used in the compensator design. It was nevertheless assumed that all the remaining seven residual modes were known so that appropriate compensation schemes could be incorporated into the control design to suppress the spillover effects from these modes.

However, the modes omitted from the evaluation model, as well as any unmodelled modes excluded from the original collection of 73 coordinates, will also cause dynamic spillover in the same manner as the residual modes. The compensator therefore must also have the ability to withstand the spillover from these modes without suffering severe performance degradation.

In practice, since the frequencies of the omitted and unmodelled modes are well beyond the control system bandwidth, most of these modes will be virtually 'invisible' to the compensator. Pre- or post-processing of the sensor and actuator signals by notch filters should minimize spillover from the modes close to or interlaced with the modelled modes, provided their frequency bands can be identified with reasonable accuracy.

Finally, hardware experimentation will provide the only reliable assessment of the robustness of the compensator design with respect to the unmodelled modes.

8.0 CONCLUDING REMARKS

We have discussed a strategy for simultaneous stationkeep and attitude control of flexible spacecraft. The method is particularly applicable to spacecraft with a constrained actuator configuration which may result in unavoidable coupling of control forces and torques. The M-SAT example considered here clearly belongs to this category, as will many third generation spacecraft with distributed sensing and actuation capabilities. Other applicable cases include large platform structures in which the actuator locations are determined more by installational constraints than by any dynamical considerations.

It has been assumed in this study that all the physical coordinates are directly measurable. These include both translational and rotational variables as well as inertial and proximity measurements. The realization of these sensor data has not been addressed in this report, and is not a problem to be lightly dismissed.

Finally, control robustness provides a critical link between theory and practice in flexible spacecraft. In Part II of this report, the control methodology presented here will be put to test through sensitivity analysis and computer simulation. The robustness of the compensator design will be quantitatively evaluated with respect to a range of parametric variations. However, it should be noted that no computer simulation can substitute for experimentation with hardware in establishing confidence in the robustness of the compensator design.

9.0 REFERENCES

1. Lang, G.B. and J.S-C. Yuan, "Reference Parameters and Control System Performance Requirements for Third Generation Spacecraft", SPAR-R.1113, October, 1982.

2. Staley, D.A., C.P. Trudel and G.B. Lang, "Third Generation Spacecraft Momentum Management Studies", DOC-CR-SP-82-017, also issued as ANCON-R.811, March, 1982.

3. Hughes, P.C., "MSAT Structural Flexibility and Control Assessment", DOC-CR-SP-81-005, also issued as Dynacon-MSAT-1, March, 1981.

4. Hughes, P.C. and G.B. Sincarsin, "MSAT Structural Dynamics Model for Control System Evaluation", DOC-CR-SP-82-022, also issued as Dynacon-MSAT-4, March, 1982.

5. "Design-Model and Evaluation-Model System Matrices for the MSAT Spacecraft", Dynacon Memo from G.B. Sincarsin to P.C. Hughes, August 25, 1982.

6. Anderson, B.D.O. and J.B. Moore, Linear Optimal Control, Prentice-Hall, Englewood Cliffs, N.J., 1971.

7. Hughes, P.C. and R.E. Skelton, "Controllability and Observability of Linear Matrix-Second-Order Systems", Trans. of ASME Journal of Applied Mechanics, Vol. 47, June, 1980, pp. 415-420.

8. Bellman, R.E., Dynamic Programming, Princeton Univ. Press, Princeton, N.J., 1957.

9. Sesak, J.R., "Suppressed Mode Damping for Model Error Sensitivity Suppression Flexible Spacecraft Controllers", AIAA Paper 80-1710, Guidance and Control Conference, August 11-13, 1980.

10. Luenberger, D.G., "An Introduction to Observers", IEEE Trans. on Automatic Control, Vol. AC-16, No. 6, December, 1971, pp. 596-602.

11. Vigneron, F.R., "Ground-Test Derived and Flight Values of Damping for a Flexible Spacecraft", ESA Symposium on Dynamics and Control of Non-Rigid Spacecraft, Frascati, Italy, May 24-26, 1976.

12. Burton, M., private communication regarding L-SAT observer design, October, 1982.

13. Yuan, J.S-C, "Design of State Estimators for the Roll and Yaw Attitudes of a Spacecraft", SPAR-TM.1567, February, 1978.

APPENDIX A

LINEAR OPTIMAL FEEDBACK CONTROL ALGORITHM

This appendix is a self-contained dissertation on a solution to the optimal control problem posed in Section 4.3. We shall invoke dynamic programming (Reference 8) to derive a control algorithm for the following problem:

Given the system equation

$$\begin{aligned} \dot{x}_c &= A_c x_c + B_c u \\ &= A_c x_c + B_{c_g} u_g + B_{c_t} u_t \end{aligned} \tag{A-1}$$

where the control inputs are defined by

$$u_t(t) = \sum_{i=0}^{K-1} u_{t_i} \delta(t - \tau_i) \tag{A-2a}$$

$$u_g(t) = u_{g_i}, \quad \tau_i \leq t < \tau_{i+1} \tag{A-2b}$$

over the time sequence

$$0 = \tau_0 < \tau_1 < \cdots < \tau_{K-1} < \tau_K = \tau$$

$$\tau_{i+1} - \tau_i = \Delta\tau, \quad i = 0, \cdots, K-1$$

The objective is to find the control sequences $\{u_{t_i}\}$ and $\{u_{g_i}\}$ to minimize the cost function

$$J = \int_0^\tau (x_c^T Q_c x_c + u_g^T R_g u_g)\, dt + \sum_{i=0}^{K-1} u_{t_i}^T R_t u_{t_i} + x_c^T(\tau) Q_{c_K} x_c(\tau) \tag{A-3}$$

where all the weighting matrices are symmetric and positive semi-definite; the control weighting matrices R_g and R_t are positive definite.

Over each sampling period, the state vector x_c can be solved from (A-1) as

$$x_c(\tau_k+t) = e^{A_c t} x_c(\tau_k) + e^{A_c t}\left[\int_0^t e^{-A_c s} ds\, B_{c_g} \qquad B_{c_t}\right]\begin{bmatrix} u_{g_k} \\ u_{t_k} \end{bmatrix}$$

for $0 \leq t \leq \Delta\tau$. Using the subscript k to simplify the notation, we can write the above equation as

$$x_c(\tau_k+t) = e^{A_c t} x_{c_k} + e^{A_c t} B_u(t)\; u_k \;, \quad 0 \leq t \leq \Delta\tau \tag{A-4}$$

where

$$B_u(t) \triangleq \left[\int_0^t e^{-A_c s} ds\; B_{c_g} \qquad B_{c_t}\right]$$

Thus, Equation (A-1) can now be discretized as

$$x_{c_{k+1}} = \bar{A}_c\, x_{c_k} + \bar{B}_c\, u_k \tag{A-5}$$

with

$$\bar{A}_c \triangleq e^{A_c \Delta\tau} \;; \qquad \bar{B}_c \triangleq e^{A_c \Delta\tau} B_u(\Delta\tau)$$

Furthermore, it can be shown that the cost function (A-3) may also be discretized and written in the form

$$J = \sum_{k=0}^{K-1} \left(x_{c_k}^T \bar{Q}\, x_{c_k} + 2 x_{c_k}^T \bar{P}\, u_k + u_k^T \bar{R}\, u_k\right) + x_{c_K}^T Q_{c_K} x_{c_K} \tag{A-6}$$

where

$$\left.\begin{aligned} \bar{Q} &\triangleq \int_0^{\Delta\tau} (e^{A_c t})^T Q_c (e^{A_c t})\, dt \\ \bar{P} &\triangleq \int_0^{\Delta\tau} (e^{A_c t})^T Q_c (e^{A_c t}) B_u(t)\, dt \\ \bar{R} &\triangleq \mathrm{diag}[R_g \Delta\tau,\; R_t] + \int_0^{\Delta\tau} (e^{A_c t} B_u(t))^T Q_c (e^{A_c t} B_u(t))\, dt \end{aligned}\right\} \tag{A-7}$$

Let us now define the following sequence of scalar functions:

$$I(x_{c_k},k) = \begin{cases} \min\limits_{u_k, u_{k+1}, \cdots u_{K-1}} \left[\sum\limits_{i=k}^{K-1} \left(x_{c_i}^T \bar{Q} x_{c_i} + 2 x_{c_i}^T \bar{P} u_i + u_i^T \bar{R} u_i \right) + x_{c_K}^T Q_{c_K} x_{c_K} \right] \\ \qquad\qquad\qquad\qquad\qquad\qquad k = 0, 1, \cdots, K-1 \\ x_{c_K}^T Q_{c_K} x_{c_K} \quad , \quad k = K \end{cases} \tag{A-8}$$

Thus, $I(x_{c_k}, k)$ represents the optimal value of J over the period $\{k, k+1, \cdots, K\}$.

Next consider the period $\{k-1, k, \cdots K\}$ over which the control sequence $\{u_k, u_{k+1}, \cdots u_{K-1}\}$ has been optimally selected. Then, according to the Principle of Optimality in dynamic programming (Reference 8), in order to obtain the optimal input at $k-1$, we must compute

$$\min_{u_{k-1}} \left\{ x_{c_{k-1}}^T \bar{Q} x_{c_{k-1}} + 2 x_{c_{k-1}}^T \bar{P} u_{k-1} + u_{k-1}^T \bar{R} u_{k-1} + I(x_{c_k}, k) \right\} \tag{A-9}$$

Furthermore, with u_{k-1} thus computed, the control sequence $\{u_{k-1}, u_k, \cdots, u_{K-1}\}$ is indeed the optimal solution over the entire period $\{k-1, k, \cdots K\}$. Hence the expression in (A-9) in fact yields $I(x_{c_{k-1}}, k-1)$. The sequence of scalar functions defined in (A-8) can now be computed from the recursive formula (solved backwards):

$$I(x_{c_k}, k) = \min_{u_k} \left\{ x_{c_k}^T \bar{Q} x_{c_k} + 2 x_{c_k}^T \bar{P} u_k + u_k^T \bar{R} u_k + I(x_{c_{k+1}}, k+1) \right\} \tag{A-10}$$

with the terminal condition

$$I(x_{c_K}, K) = x_{c_K}^T Q_{c_K} x_{c_K} \tag{A-11}$$

This sequence will then enable us to compute the optimal control sequence as we shall presently show.

Judging from the terminal condition (A-11), one can conjecture that the sequence $I(x_{c_k}, k)$ has the general form

$$I(x_{c_k}, k) = x_{c_k}^T Q_k x_{c_k} \tag{A-12}$$

where Q_k is symmetric with

$$Q_K = Q_{c_K}$$

The recursive equation (A-10) now becomes

$$x_{c_k}^T Q_k x_{c_k} = \min_{u_k} \left\{ x_{c_k}^T \bar{Q} x_{c_k} + 2 x_{c_k}^T \bar{P} u_k + u_k^T \bar{R} u_k + x_{c_{k+1}}^T Q_{k+1} x_{c_{k+1}} \right\}$$

Substitution of (A-5) for $x_{c_{k+1}}$ yields

$$x_{c_k}^T Q_k x_{c_k} = \min_{u_k} \left\{ x_{c_k}^T \left[\bar{Q} + \bar{A}_c^T Q_{k+1} \bar{A}_c \right] x_{c_k} + u_k^T \left[\bar{R} + \bar{B}_c^T Q_{k+1} \bar{B}_c \right] u_k + 2 x_{c_k}^T \left[\bar{P} + \bar{A}_c^T Q_{k+1} \bar{B}_c \right] u_k \right\} \tag{A-13}$$

The optimal solution on the right hand side is clearly given by

$$\begin{aligned} u_k &= - \left[\bar{R} + \bar{B}_c^T Q_{k+1} \bar{B}_c \right]^{-1} \left[\bar{P} + \bar{A}_c^T Q_{k+1} \bar{B}_c \right]^T x_{c_k} \\ &\triangleq F_k \, x_{c_k} \end{aligned} \tag{A-14}$$

The matrix inverse exists since it is symmetric and positive definite. Also, balancing the terms on each side of (A-13) with the optimal control (A-14) inserted, we get

$$Q_k = \bar{Q} + \bar{A}_c^T Q_{k+1} \bar{A}_c + \left[\bar{P} + \bar{A}_c^T Q_{k+1} \bar{B}_c \right] F_k \tag{A-15}$$

with

$$Q_K = Q_{c_K} \tag{A-16}$$

Given Q_{c_K} is symmetric, it can easily be shown that every other Q_k is also symmetric. Equation (A-14) to (A-16) thus provide the recursive expressions for computing the optimal feedback gain matrix F_k.

We can now summarize the optimal control algorithm as follows:

(a) Begin at $k=K$, set

$$Q_K = Q_{c_K}$$

(b) For each $k = K-1, \ldots, 0$

i) Compute F_k from Q_{k+1} as given in (A-14)

ii) Update Q_{k-1} from F_k and Q_k as given in (A-15) (except at $k=0$).

(c) The optimal value of the cost function (A-6) is given by

$$I(x_{c_0}, 0) = x_{c_0}^T Q_0 \, x_{c_0} \qquad \text{(A-17)}$$

This algorithm can be conveniently implemented on a digital computer.

APPENDIX B

A COMPARISON OF FULL-ORDER AND REDUCED-ORDER OBSERVERS

We present here a trade-off study of full-order versus reduced-order observers with respect to dynamic spillover effects. Consider the following system

$$\dot{x}_c = A_c x_c + B_c u \tag{B-1a}$$

$$\dot{x}_R = A_R x_R + B_R u \tag{B-1b}$$

$$y = C_c x_c + C_R x_R \tag{B-1c}$$

where x_c and x_R are the controlled and residual states, respectively. Only x_c is to be estimated from the output y which is a linear combination of x_c and x_R. We further assume that the system (B-1) is completely controllable and completely observable.

Suppose the control law is given in the linear feedback form

$$u = F \hat{x}_c \tag{B-2}$$

where $\hat{x}_c$ is an estimate of x_c. Denote the estimation error as

$$\varepsilon \triangleq \hat{x}_c - x_c$$

Then (B-2) is equivalent to

$$u = F x_c + F \varepsilon \tag{B-3}$$

The closed-loop system is thus described by the equations

$$\dot{x}_c = (A_c + B_c F) x_c + B_c F \varepsilon \tag{B-4a}$$

$$\dot{x}_R = A_R x_R + B_R F x_c + B_R F \varepsilon \tag{B-4b}$$

Controllability ensures that all the eigenvalues of $(A_c + B_c F)$ are freely assignable by a suitable choice of F to stabilize the controlled states x_c. However, as we shall show presently, the estimation error will also influence system stability.

Consider first the full-order observer which is given in the classical form (Reference 10) by

$$\mathring{\hat{x}}_c = (A_c - KC_c)\hat{x}_c + B_c u + Ky \qquad \text{(B-5)}$$

It is not difficult to show that the error dynamics are governed by the equation

$$\dot{\varepsilon} = (A_c - KC_c)\varepsilon + KC_R x_R \qquad \text{(B-6)}$$

Observability guarantees that all the eigenvalues of $(A_c - K C_c)$ are freely assignable by the choice of an appropriate gain matrix K to stabilize the error dynamics.

The closed-loop system with the full-order observer (B-5) in the loop is now described by the following equations

$$\begin{bmatrix} \dot{x}_c \\ \dot{\varepsilon} \\ \dot{x}_R \end{bmatrix} = \begin{bmatrix} A_c + B_c F & B_c F & 0 \\ 0 & A_c - KC_c & KC_R \\ B_R F & B_R F & A_R \end{bmatrix} \begin{bmatrix} x_c \\ \varepsilon \\ x_R \end{bmatrix} \qquad \text{(B-7)}$$

Notice that stability is no longer assured due to the presence of the spillover terms $B_R F$ and KC_R.

On the other hand, in order to restore system stability, it suffices to remove either one of the spillover terms, that is

$$KC_R = 0 \qquad \text{(B-8a)}$$

or

$$B_R F = 0 \tag{B-8b}$$

Thus, Conditions (B-8) represent additional design constraints on the gain matrices F and K.

We now consider the reduced-order observer. Ignore the residual state x_R for the moment and let the output be given simply as

$$y = C_c x_c$$

Also assume C_c has full rank and that

$$\text{rank } C_c = d(y) < d(x_c)$$

which is usually the case in practice. We can augment another matrix C_{c_1} to C_c so that the square matrix

$$M = \begin{bmatrix} C_c \\ \hdashline C_{c_1} \end{bmatrix} \tag{B-9}$$

now has a rank of $d(x_c)$ and is invertible. We can now define a set of artificial outputs

$$y_a = C_{c_1} x_c$$

so that

$$\begin{bmatrix} y \\ \hdashline y_a \end{bmatrix} = \begin{bmatrix} C_c \\ \hdashline C_{c_1} \end{bmatrix} x_c = M x_c$$

Since M is invertible, we can now estimate x_c by

$$\hat{x}_c = M^{-1} \begin{bmatrix} y \\ \hdashline \hat{y}_a \end{bmatrix} \tag{B-10}$$

provided an estimate of y_a is also available. The problem is thus reduced to finding an estimator for y_a. The order for such an observer is given by

$$d(y_a) = d(x_c) - d(y)$$

The details of the design of a reduced-order observer can be found in most standard control theory textbooks, and will not be repeated here. We simply list the equations as

$$\hat{y}_a = v + K y \tag{B-11a}$$

$$\dot{v} = (A_{22} - K A_{12}) v + \left[(A_{22} - K A_{12}) K + (A_{21} - K A_{11}) \right] y + B_a u \tag{B-11b}$$

where the indexed matrices are derived from the following partitioned matrices

$$M A_c M^{-1} = \left[\begin{array}{c|c} A_{11} & A_{12} \\ \hline A_{21} & A_{22} \end{array} \right] \qquad M B_c = \left[\begin{array}{c} 0 \\ \hline B_a \end{array} \right] \tag{B-12}$$

If we define the estimation error for y_a as

$$\varepsilon_y \triangleq \hat{y}_a - y_a$$

then it can be shown that the error dynamics are described by the equation

$$\dot{\varepsilon}_y = (A_{22} - K A_{12}) \varepsilon_y + \left[K C_R A_R + (A_{21} - K A_{11}) C_R \right] x_R + K C_R B_R u \tag{B-13}$$

Once again, observability ensures that the observer gain matrix K may be freely chosen to stabilize the matrix $(A_{22} - K A_{12})$.

The feedback control (B-2) is now given by

$$u = F\hat{x}_c = FM^{-1}\begin{bmatrix} y \\ \hdashline \bar{y}_a \end{bmatrix} = FM^{-1}\left\{ \begin{bmatrix} C_c \\ \hdashline C_{c_1} \end{bmatrix} x_c + \begin{bmatrix} C_R x_R \\ \hdashline \varepsilon_y \end{bmatrix} \right\}$$

$$= F x_c + FM^{-1}\begin{bmatrix} C_R x_R \\ \hdashline \varepsilon_y \end{bmatrix} \qquad \text{(B-14)}$$

Partition FM^{-1} as

$$FM^{-1} = [F_1 \mid F_2]$$

Substituting (B-13) and (B-14) into the system equations (B-1), we get the following closed-loop system equations

$$\begin{bmatrix} \dot{x}_c \\ \dot{\varepsilon}_y \\ \dot{x}_R \end{bmatrix} = \begin{bmatrix} A_c + B_c F & B_c F_2 & B_c F_1 C_R \\ K C_R B_R F & A_{22} - K A_{12} + K C_R B_R F_2 & K C_R (A_R + B_R F_1 C_R) + (A_{21} - K A_{11}) C_R \\ B_R F & B_R F_2 & A_R + B_R F_1 C_R \end{bmatrix} \begin{bmatrix} x_c \\ \varepsilon_y \\ x_R \end{bmatrix} \qquad \text{(B-}$$

In comparison to Equation (B-7) for the full-order observer case, it is clear that there is now a much higher degree of dynamic interaction from the spillover terms. In fact, the removal of observation spillover (KC_R) alone is no longer sufficient to guarantee closed-loop stability.

In conclusion, there is a definite trade-off between observer complexity and performance sensitivity. In the case of flexible spacecraft, many of the design parameters are highly uncertain to begin with, while others could vary considerably over the life of the spacecraft. Robustness in the compensator has become an important design criterion. However, with the declining cost of microprocessor technology, design complexity, while still a major concern, is no longer as critical an issue as it was before. It is therefore recommended that only full-order observers be considered for flexible spacecraft.

APPENDIX C

DESIGN OF OBSERVER WITH SELECTIVE SPILLOVER COMPENSATION

In this appendix, we discuss a method for extending the observer bandwidth through active spillover compensation.

Consider the following system equations

$$\dot{x}_c = A_c x_c + B_c u \quad ; \quad d(x_c) = n_c \tag{C-1a}$$

$$y = C_c x_c + C_R x_R \quad ; \quad d(y) = m \; , \; d(x_R) = n_R \tag{C-1b}$$

where x_c and x_R denote the controlled and residual states, respectively; y is the output vector. Assume the system is completely observable. Then a full-order observer is given by

$$\dot{\hat{x}}_c = (A_c - K C_c)\hat{x}_c + B_c u + K y \tag{C-2}$$

where the error dynamics are described by the equations

$$\varepsilon \triangleq \hat{x}_c - x_c$$

$$\dot{\varepsilon} = (A_c - K C_c)\varepsilon + K C_R x_R \tag{C-3}$$

Observability ensures that the gain K may be freely chosen to stabilize the matrix ($A_c - K C_c$) so that the estimation error remains bounded so long as x_R is bounded.

Still, for the sake of closed-loop stability, it is desirable to prevent as much of the contents of x_R from leaking through the observer as possible. A simple method to achieve this is to limit the bandwidth of the observer to exclude the dominant frequencies present in x_R . However, the observer response that results may not be acceptable to the overall control objective. In this case, the dynamic spillover must be actively compensated in order to allow extension of the observer bandwidth.

For complete elimination of the observation spillover, it is not difficult to see that the gain K must be selected so that

(a) $KC_R = 0$ (C-4a)

(b) ($A_c - KC_c$) is stabilized (C-4b)

A necessary condition for (C-4a) is

$$m > n_R$$

that is, the number of outputs must exceed the number of residual states. Due to the usually large number of residual states present in a flexible spacecraft, this condition would demand an excessive number of sensors and thus becomes practically infeasible.

On the other hand, suppose that only the spillover contributions from certain specific residual states are to be suppressed, say

$$\{ x_{R_1}, \cdots, x_{R_p} \}$$

where

$$p < \min \{ m, n_R \} \qquad \text{(C-5)}$$

Then, from the control point of view, it may be sufficient that only the corresponding columns in KC_R :

$$\{ KC_{R_1}, KC_{R_2}, \cdots, KC_{R_p} \}$$

be nulled. In the case of flexible spacecraft, all the known residual states are identifiable by their frequencies. One can therefore simply pick out those modes whose frequencies fall within the observer bandwidth.

The conditions (C-4) can now be modified as

(a) $KC_{R_i} = 0 \quad , i=1, \cdots, p$ (C-6a)

(b) ($A_c - KC_c$) is stabilized. (C-6b)

By virtue of (C-5) and assuming the columns c_{R_i} are linearly independent, we know that there exists an $(m-p) \times m$ matrix $\bar{K}$ with full rank ($m-p$) such that

$$\bar{K} c_{R_i} = 0 \quad , \quad i = 1, \cdots, p \qquad \text{(C-7)}$$

Furthermore, any K satisfying (C-6a) will necessarily be of the form

$$K = \Lambda \bar{K}$$

where the elements of Λ express the rows of K as linear combinations of the rows in $\bar{K}$. Condition (C-6b) is thus reduced to the problem of finding Λ to stabilize the matrix ($A_c - \Lambda \bar{K} C_c$). This can be done if and only if ($\bar{K} C_c$, A_c) is observable.

Note that the matrix $\bar{K} C_c$ has effectively replaced the original output matrix C_c . Also, since $\bar{K} C_c$ now has only ($m-p$) rows, one would expect the system to be somewhat 'less observable' than before. This will be reflected in an additional constraint on p , the number of suppressed residual states, as we shall demonstrate next.

As illustration, consider the case where the controlled states comprise both rigid and elastic variables, i.e.,

$$x_c^T = [x_r^T , x_e^T]$$

and

$$A_c = \left[\begin{array}{cc|cc} 0 & I & \multicolumn{2}{c}{\multirow{2}{*}{0}} \\ 0 & 0 & & \\ \hline \multicolumn{2}{c|}{\multirow{2}{*}{0}} & 0 & I \\ & & -\Omega^2 & -2\zeta\Omega \end{array} \right]$$

Assume that the output vector can be separated into two groups:

$$y = \begin{bmatrix} y_r \\ \hline y_e \end{bmatrix} = \left[\begin{array}{c|c} C_r & C_e \\ \hline 0 & \end{array}\right] \begin{bmatrix} x_r \\ \hline x_e \end{bmatrix} + C_R x_R$$

where y_e consists of only elastic modal measurements. Assume further that only the position variables in the rigid states are measureable so that

$$C_r = [C_{r_p} \mid 0]$$

where C_{r_p} is a square matrix with full rank, i.e.,

$$\text{rank } C_{r_p} = d(y_r) = \tfrac{1}{2} d(x_r)$$

The above assumptions clearly fit the system model used earlier in this report (cf. Table 3-1).

Now partition the matrix $\bar{K}$ of (C-7) as

$$\bar{K} = [\bar{K}_r \mid \bar{K}_e]$$

Thus

$$\bar{K}C_c = [\bar{K}_r C_r \mid \bar{K} C_e]$$

It can be shown that ($\bar{K}C_c$, A_c) is observable if and only if

(a) $\text{rank } \bar{K}_r C_{r_p} = \tfrac{1}{2} d(x_r) = d(y_r)$ (C-8a)

(b) $\bar{K}C_e$ contains no zero column. (C-8b)

Clearly, a necessary condition for (C-8a) is

$$(m-p) \geq d(y_r)$$

Since

$$m = d(y_r) + d(y_e)$$

The above condition becomes

$$p \leq d(y_e) \tag{C-9}$$

In other words, the number of suppressed residual states cannot be more than the number of elastic modal measurements.

OPTIMAL STATIONKEEP AND ATTITUDE
CONTROL OF FLEXIBLE SPACECRAFT